Moderne Anwendungen der Festkörper-NMR-Spektroskopie in der heterogenen Katalyse

Michael Hunger

Institut für Technische Chemie

Universität Stuttgart

BASF

Ludwigshafen

12. Mai 2016

Most abundant isotopes with nuclear spin

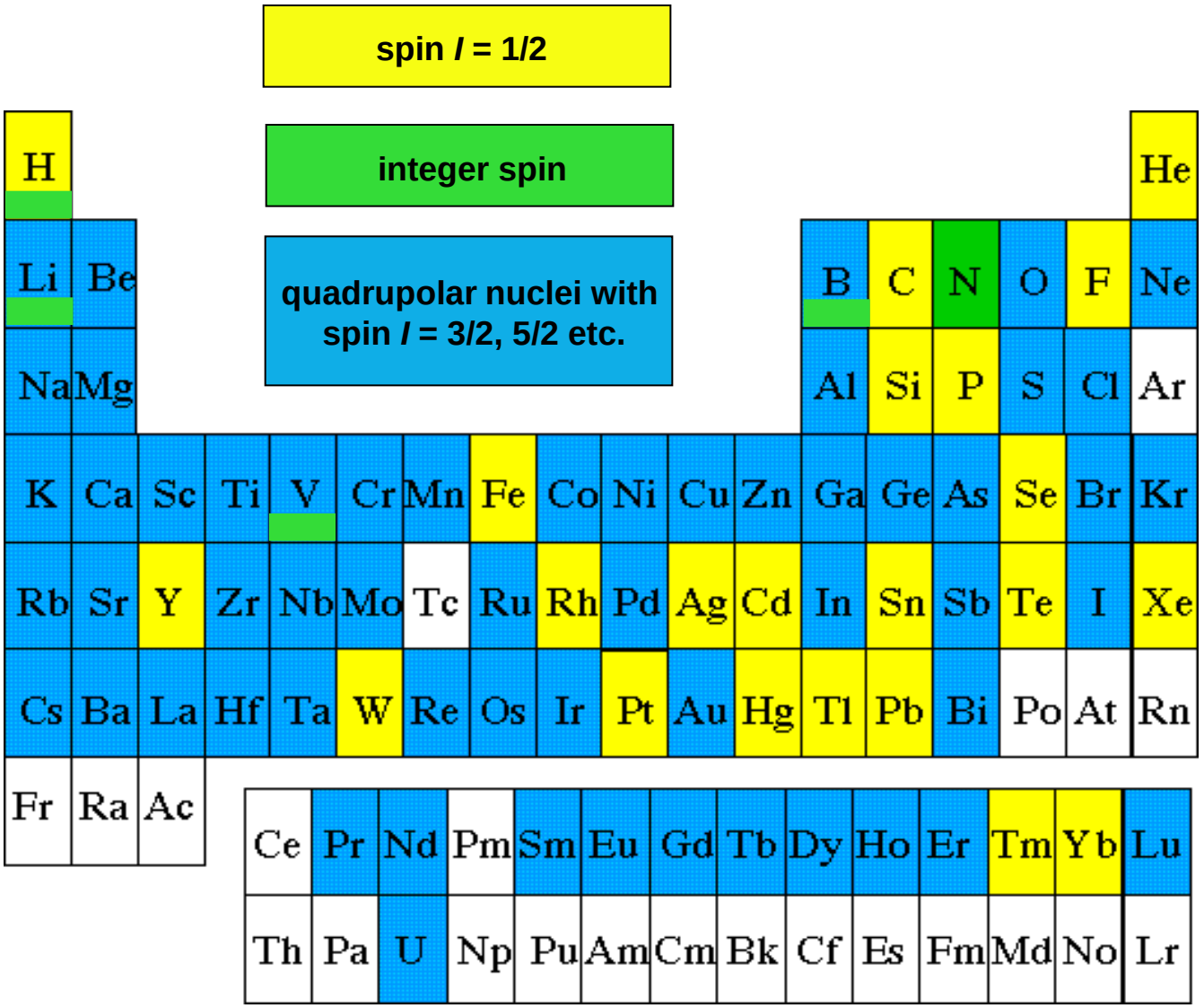

Isotopes interesting for solid-state NMR in heterogeneous catalysis

interesting isotopes (nuclear spin, relative sensitivity in comparison with ^{1}H)

^{1}H (1/2, 1.00), ^{2}H (1, 1.4×10^{-6})

^{13}C (1/2, 1.8×10^{-4}), ^{15}N (1/2, 3.8×10^{-6})

^{31}P (1/2, 6.6×10^{-2})

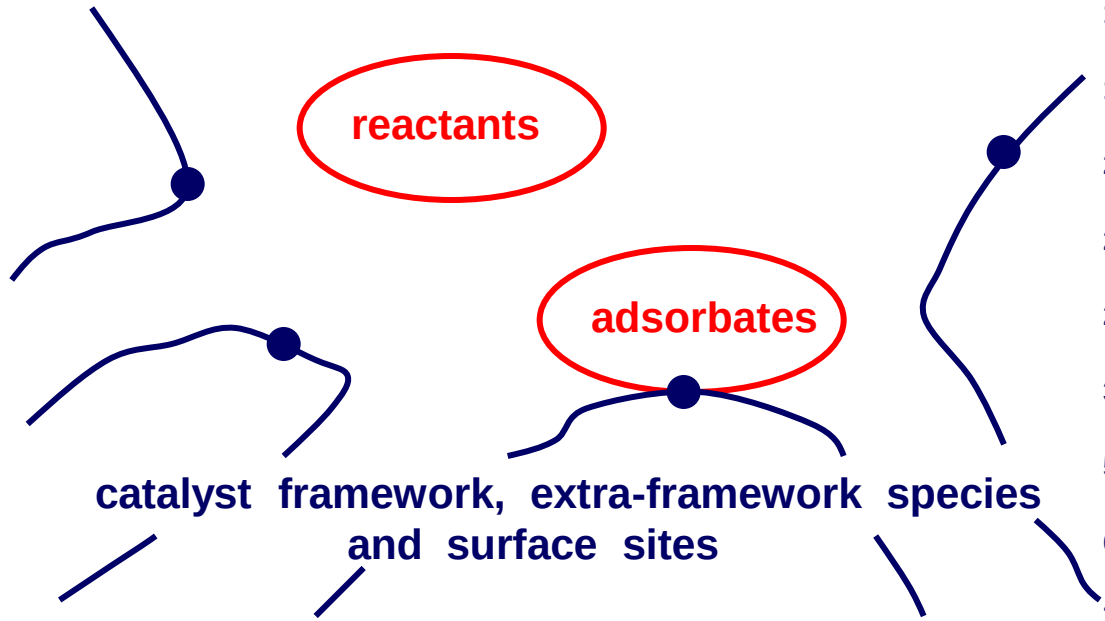

^{7}Li (3/2, 0.27)

^{11}B (3/2, 0.13)

^{17}O (5/2, 1.1×10^{-5})

^{23}Na (3/2, 9.2×10^{-2})

^{27}Al (5/2, 0.21)

^{29}Si (1/2, 3.7×10^{-4})

^{31}P (1/2, 6.6×10^{-2})

^{51}V (7/2, 0.38)

^{67}Zn (5/2, 1.2×10^{-2})

^{71}Ga (3/2, 5.6×10^{-2})

^{133}Cs (7/2, 4.7×10^{-2})

Specific problems of solid-state NMR spectroscopy

Magnetization M_0, Curie's law:

$$M_0 = \frac{N\,\gamma^2\,h^2\,I\,(I+1)\,B_0}{(2\pi)^2\,3\,k_B\,T}$$

detection limit of solid-state NMR is ca. N = 10 µmol spins per gram for ^{1}H nuclei at room temperature

magnetization M_0 decreases with increasing temperature T

broadening of NMR signals due to internal solid-state interactions

most important solid-state interactions:

H_{CSA} : anisotropic shielding of the magnetic field due to the anisotropic electron density in the local structure of the resonating nuclei; $\mathcal{F}$ {LP$^{(2)}$} — $\Delta\nu_{CSA}$ up to 50 kHz or ca. 100 ppm

H_{DI} : dipolar interaction with magnetic dipole moments of neighboring spins in the local structure; $\mathcal{F}$ {LP$^{(2)}$} — $\Delta\nu_{DI}$ up to 100 kHz or ca. 200 ppm

H_{QI} : quadrupolar interaction of the electric quadrupole moment of nuclei with spin I = 3/2, 5/2 etc. with electric field gradients; $\mathcal{F}$ {LP$^{(2)}$ + LP$^{(4)}$} — $\Delta\nu_Q$ up to 20 MHz or ca. 40000 ppm

Techniques of solid-state NMR spectroscopy

spin *I* = 1/2 :

magic angle spinning (MAS)

$\nu_{CSA,\ DI,\ QI1} = \mathcal{F}\ \{(3\cos^2\Theta - 1)/2\}$

$\rightarrow\ \Theta = 54.7^o$

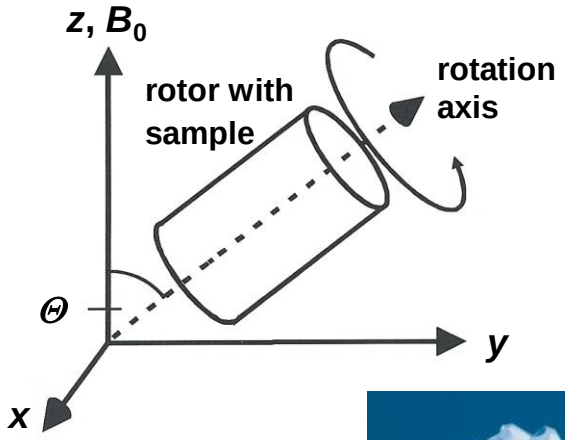

spin *I* = 3/2, 5/2 etc. :

double oriented rotation (DOR)

$\nu_{QI2} = \mathcal{F}\ \{(35\cos^4\Theta - 30\cos^2\Theta + 3)/8\}$

$\rightarrow\ \Theta = 30.6^o$

$\Theta = 70.1^o$

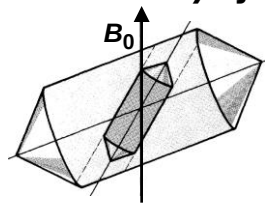

multiple-quantum MAS NMR (MQMAS)

- excitation of three- and five-quantum transitions
- recording of a spin-echo free of anisotropic contributions

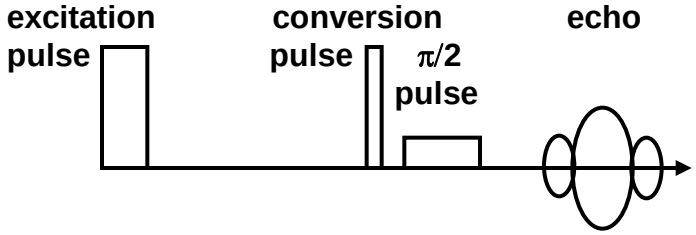

J. Amoureux et al., J. Magn. Reson A 123 (1996) 116

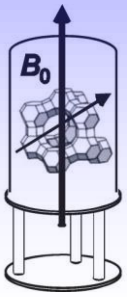

Solid-state NMR of solid catalysts

I. Synthesis of catalysts ⟷
- nature and local structure of framework atoms
- framework defects, amorphous phases and impurities

↓

II. Framework modification ⟷
- incorporation and release of framework atoms
- nature and location of extra-framework species and cations
- anchoring of organic compounds

↓

III. Tailoring of surface sites ⟷
- number, strength, and accessibility of Brønsted acid sites
- presence and strength of base sites
- presence of Lewis acid sites

↓

IV. Catalytic investigations ⟷
- adsorbate complexes and intermediates formed on catalysts
- reaction mechanisms
- reasons of catalyst deactivation

↓

topics I to III

I. Synthesis of catalysts

I. Synthesis of catalysts

synthesis of zeolite [Ga,Al]Beta by steam-assisted dry-gel conversion (SAC)

structure of zeolite Beta (BEA)

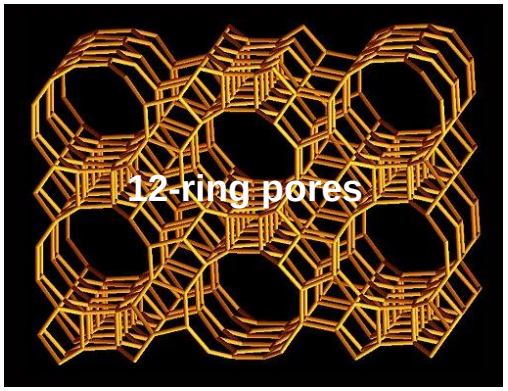

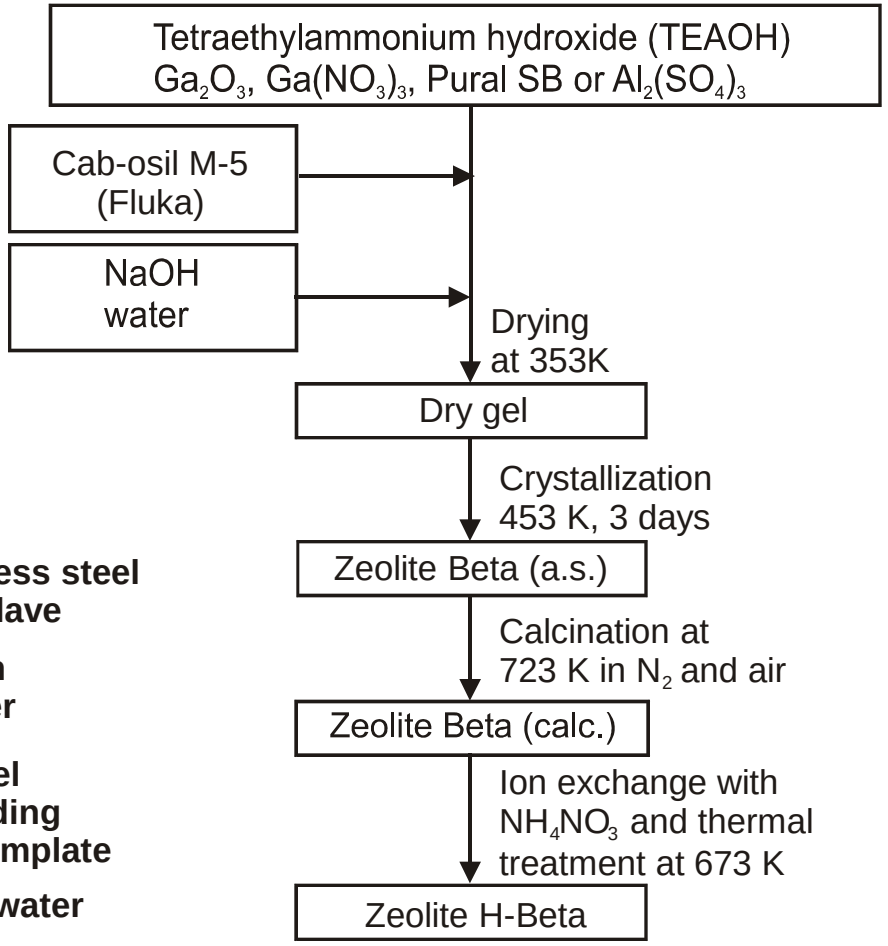

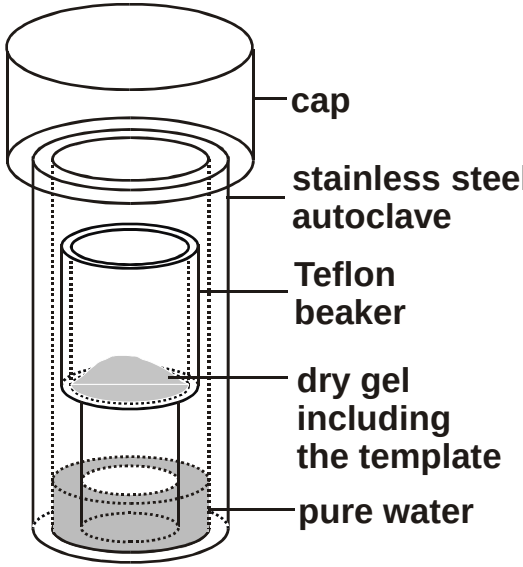

autoclave volume:
110 cm^3
Teflon beaker:
14.5 cm^3

A. Arnold et al., Microporous Mesoporous Mater. 62 (2003) 97.

I. Synthesis of catalysts

synthesis of zeolite [Ga,Al]Beta by steam-assisted dry-gel conversion (SAC)

^{29}Si MAS NMR spectra recorded after different SAC times

B_0 = 9.4 T, ν_0 = 79.5 MHz

SAC time of 16 h

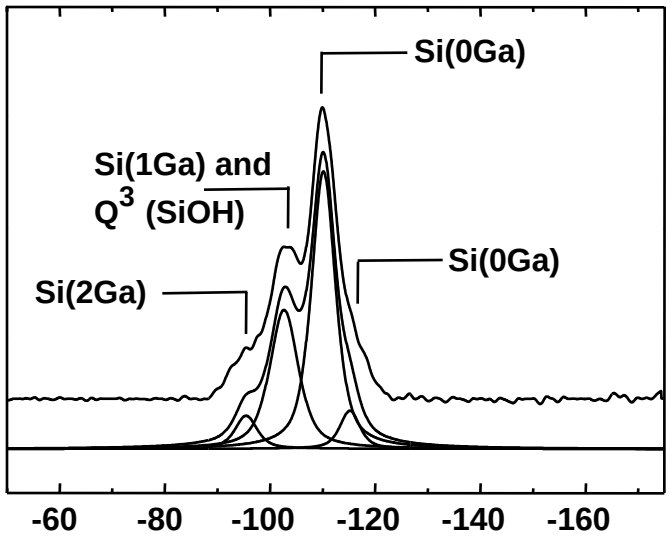

SAC time of 65 h

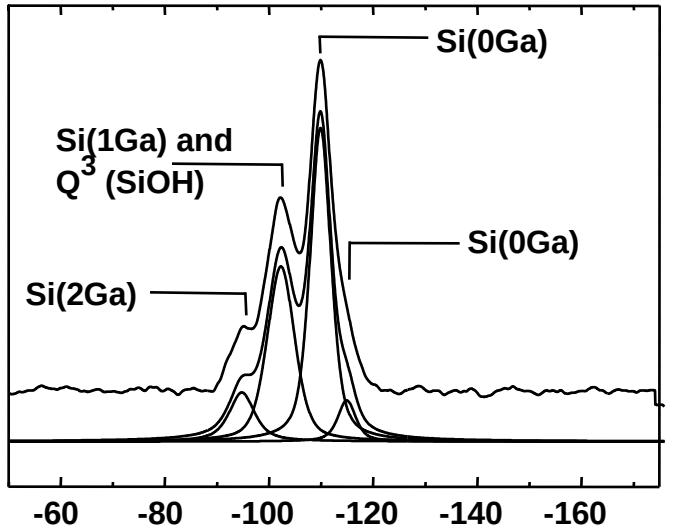

Si(1Ga): **Q^4 framework silicon with one Si-O-Ga and three Si-O-Si bonds, Si(3Si,1Ga), at -101 ppm is overlapped by the Q^3 signal, Si(3Si,1OH), at *ca.* -103 ppm**

Si(2Ga): **framework silicon with two Si-O-Ga and two Si-O-Si bonds, Si(2Si,2Ga), at -95 ppm**

Q^4: Si(3Si,1Ga)

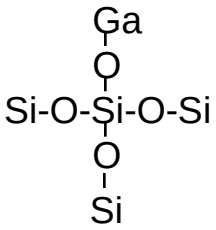

A. Arnold et al., Microporous Mesoporous Mater. 62 (2003) 97.

I. Synthesis of catalysts

synthesis of zeolite [Ga,Al]Beta by steam-assisted dry-gel conversion (SAC)

^{71}Ga MAS NMR spectra (spin *I* = 3/2) recorded after different SAC times

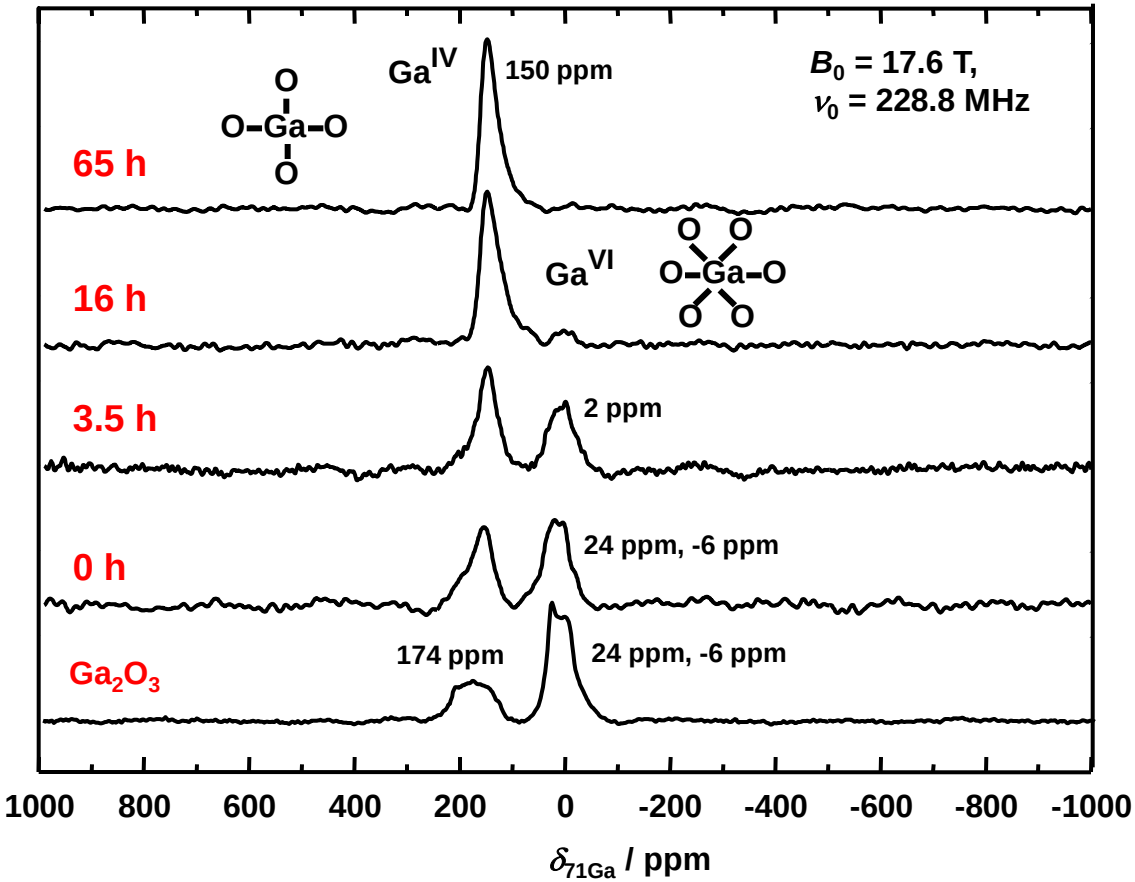

gallium coordination:

Ga^{IV} /%	Ga^{VI} /%
100	0
93	7
58	42
45	55
34	66

complete tetrahedral oxygen coordination of gallium atoms after a SAC time of 65 h

A. Arnold et al., Microporous Mesoporous Mater. 62 (2003) 97.

I. Synthesis of catalysts

synthesis of zeolite [Ga,Al]Beta by steam-assisted dry-gel conversion (SAC)

^{71}Ga MQMAS NMR spectroscopy (spin *I* = 3/2) of [Ga]Beta sample obtained at 65 h

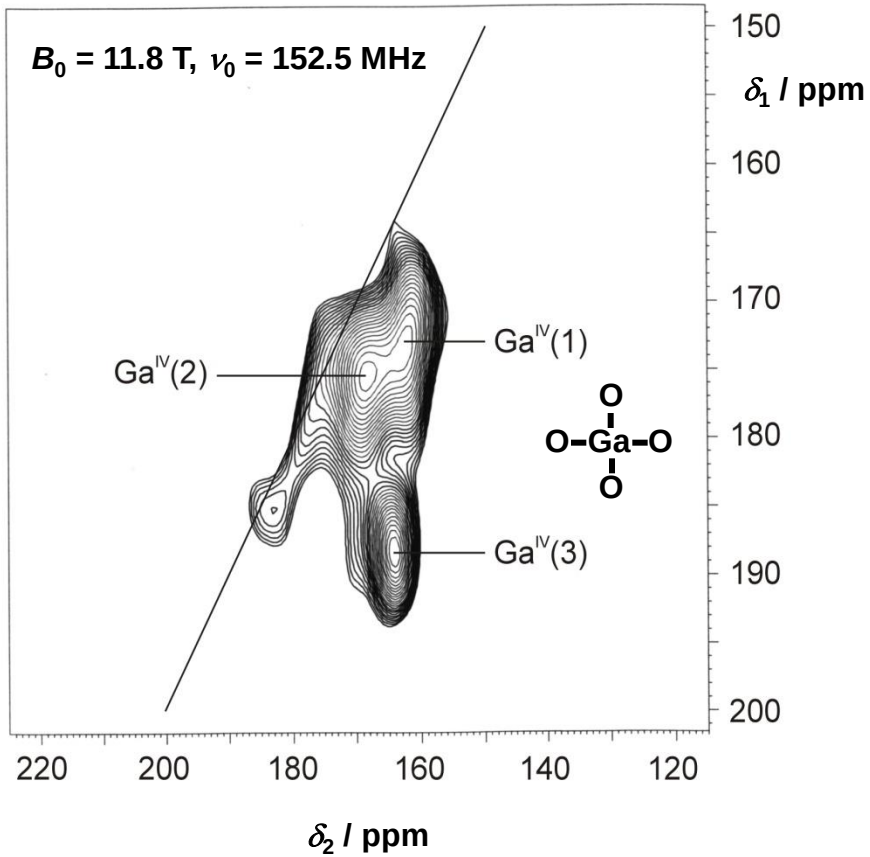

Ga^{IV}(1, 2):
framework gallium species,
SOQE = 2.2 and 1.8 MHz,
δ_{iso} = 172 and 168 ppm

Ga^{IV}(3):
extra-framework gallium species or amorphous phases,
SOQE = 4.7 MHz,
δ_{iso} = 176 ppm

***SOQE*: second-order quadrupole effect parameter, strength of quadrupolar interaction**

A. Arnold et al., Microporous Mesoporous Mater. 62 (2003) 97.

I. Synthesis of catalysts

synthesis of flame-derived silica-alumina with different aluminum contents

preparation of flame-made silica-alumina (SA) catalysts:

dissolving aluminum(III) acetylacetonate and tetraethoxysilane in a 1:1 (vol%) mixture of acetic acid and methanol

this solution was pumped through a capillary with 5 ml/min and nebulized with 5 l/min O_2

the spray was ignited by a methane/ oxygen flame (1.5/0.9 L/min) resulting in an approximately 6 cm long flame

particles (*ca.* 20 nm) were collected on a cooled Whatman GF6 filter

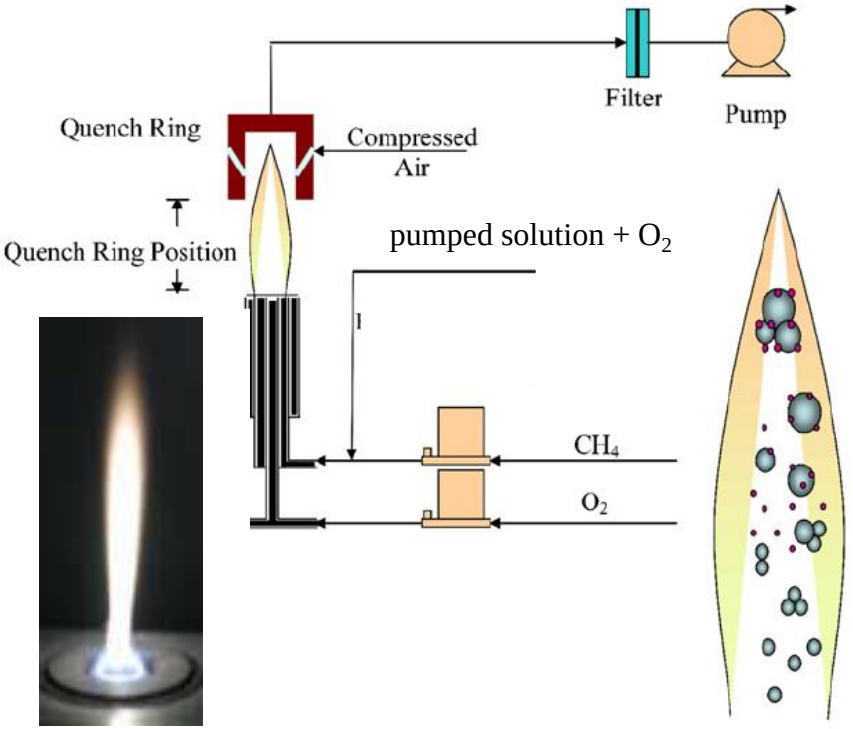

J. Huang et al., Angew. Chem. Int. Ed. 49 (2010) 7776.

I. Synthesis of catalysts

synthesis of flame-derived silica-alumina with different aluminum contents

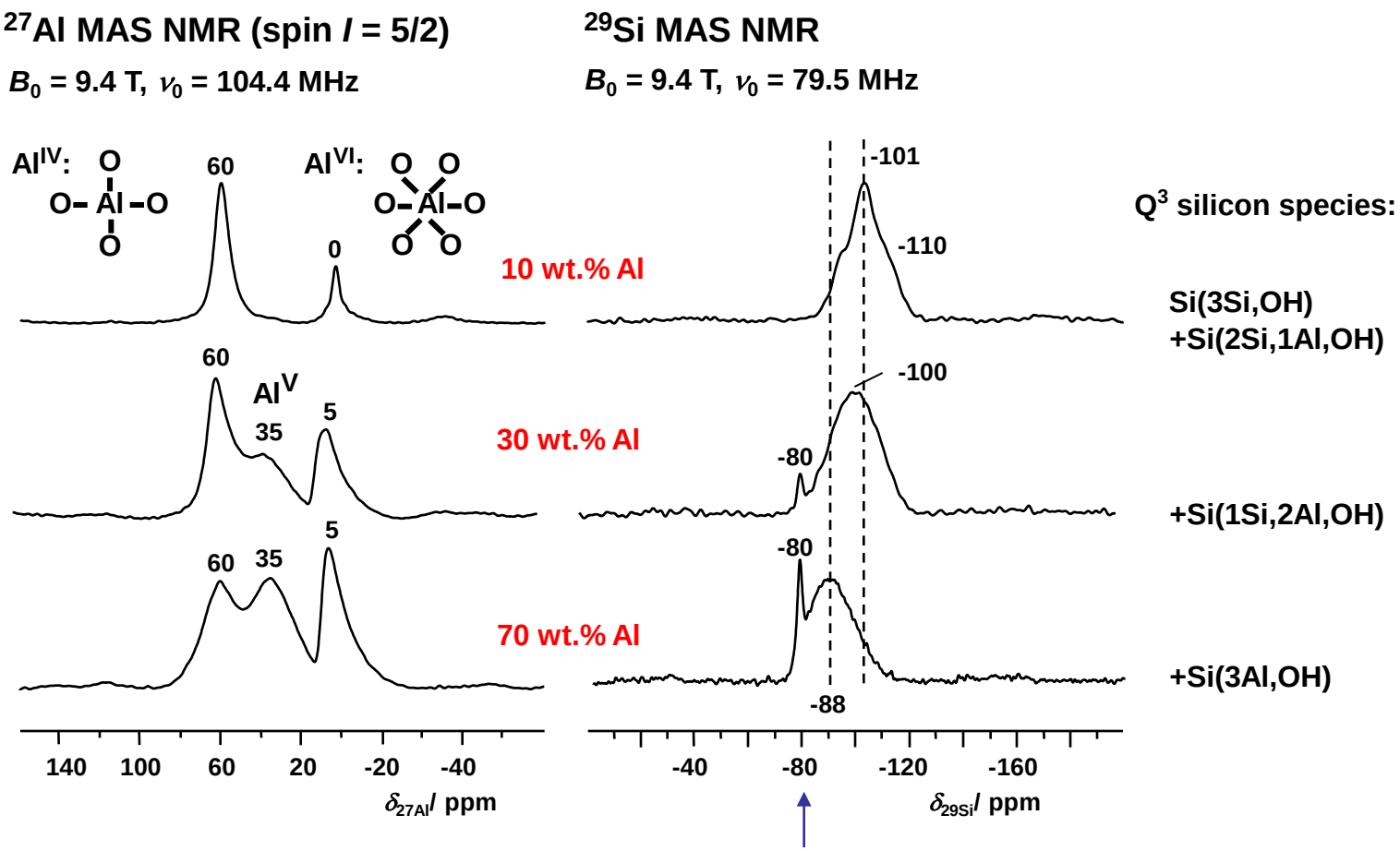

observation of minor andalusite phases (Al_2SiO_5) with δ_{29Si} = -79.8 ppm (M. Mägi *et al.*, J. Phys. Chem. 88 (1984) 1518) possible

J. Huang et al., Angew. Chem. Int. Ed. 49 (2010) 7776.

I. Synthesis of catalysts

synthesis of flame-derived silica-alumina with different aluminum contents

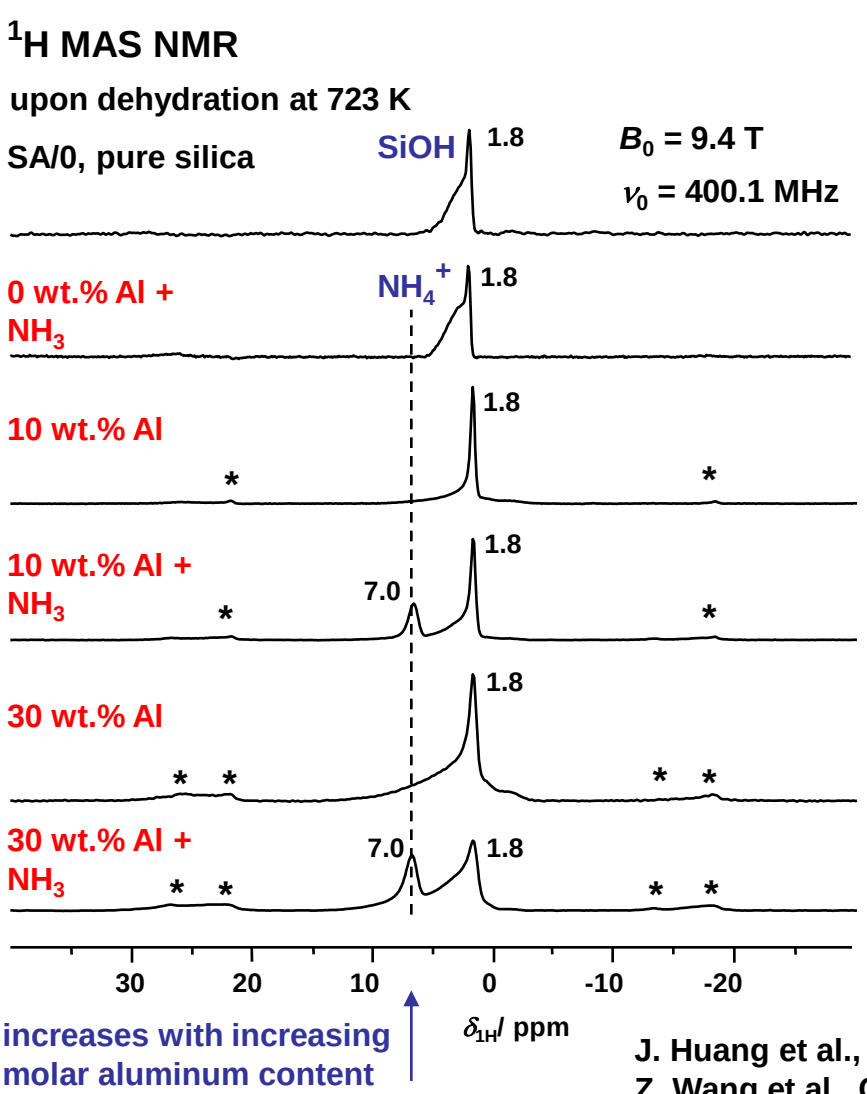

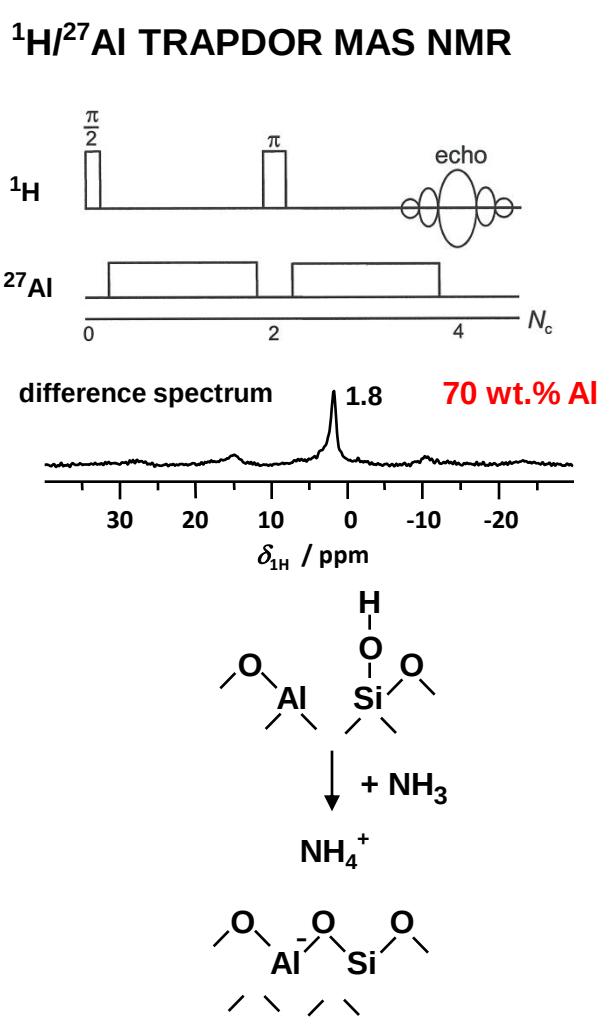

J. Huang et al., Angew. Chem. Int. Ed. 49 (2010) 7776.
Z. Wang et al., Catal. Sci. Technol. 5 (2015) 2788.

II. Framework modification

II. Framework modification

dealumination of zeolite H,Na-Y by steaming

structure of zeolite Y (FAU)

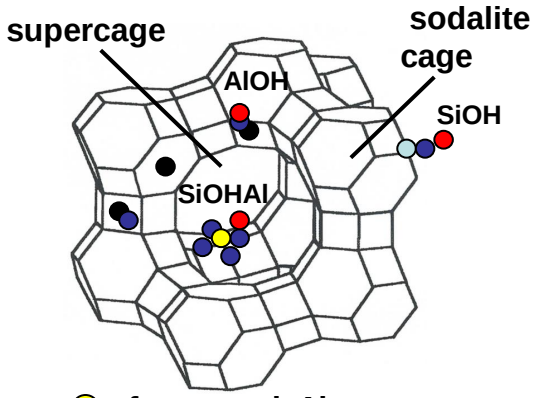

dealumination procedure

commercial zeolite Na-Y (n_{Si}/n_{Al} = 2.7)

→ ammonium exchange (93%) →

steaming at 748 K under flowing nitrogen (100 ml/min) with a water vapor pressure of 7.4-81.5 kPa

→

dealuminated zeolite deH,Na-Y/31.1-81.5 (n_{Si}/n_{Al} = 3.6-6.0)

→

transfer into gas-tight MAS NMR rotor without rehydration

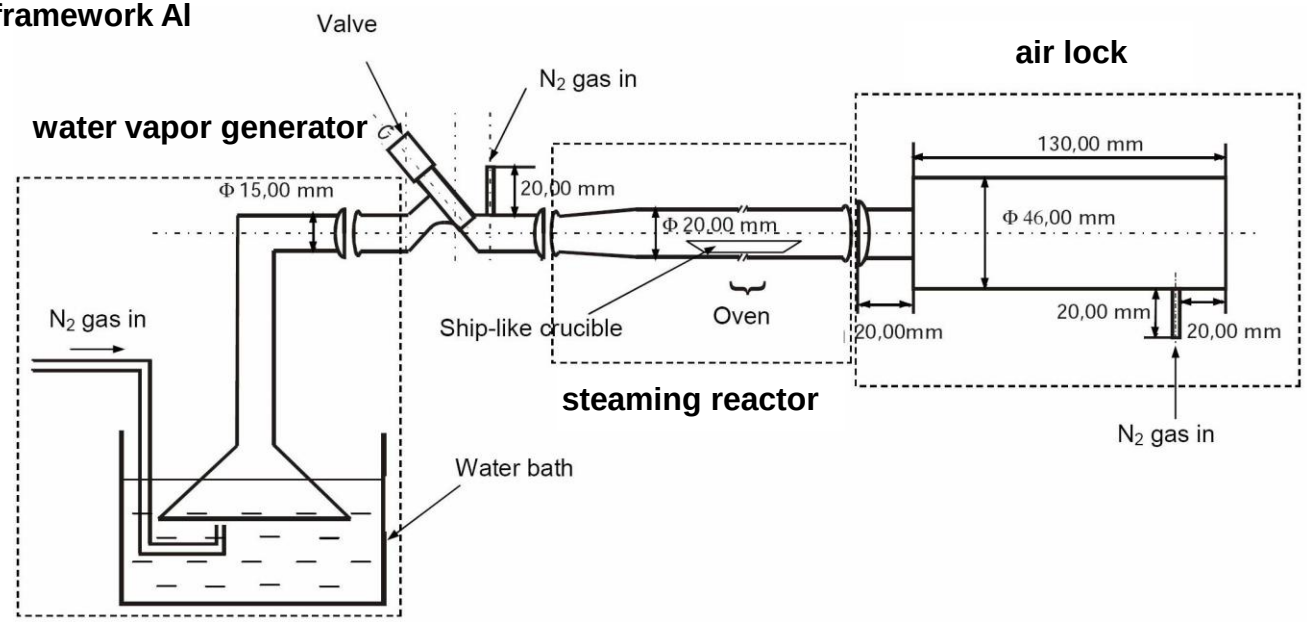

II. Framework modification

dealumination of acidic zeolites by steaming

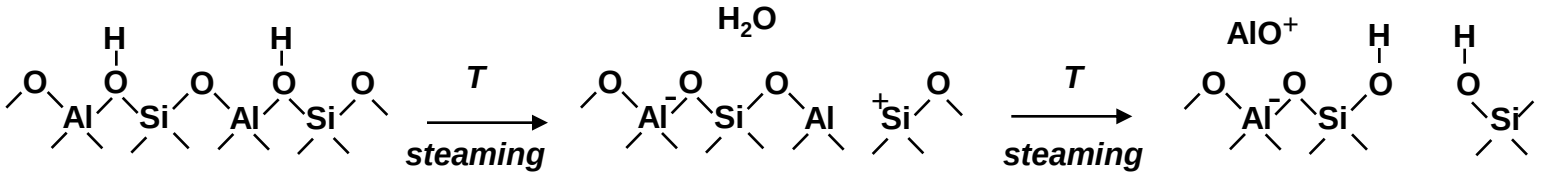

^{29}Si MAS NMR spectroscopy of zeolites H,Na-Y (left) and deH,Na-Y/31.1 (right)

B_0 = 9.4 T, ν_0 = 79.5 MHz

hydrated state

dehydrated and loaded with NH_3

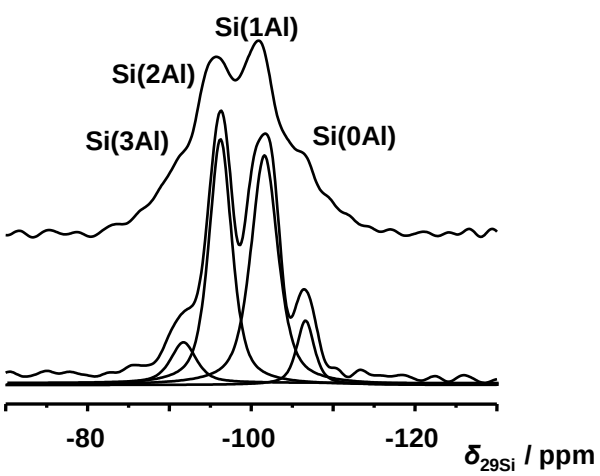

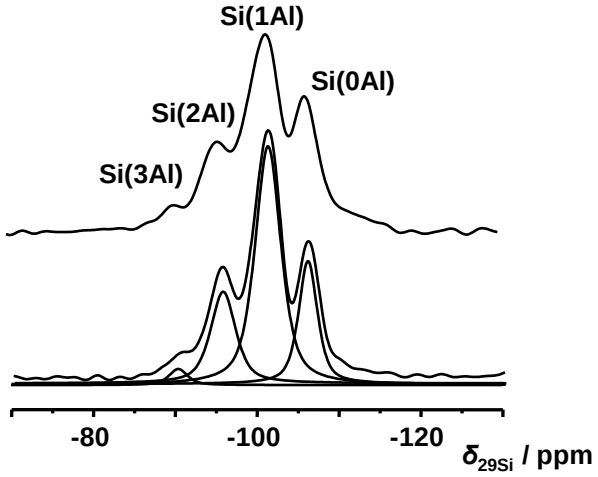

$$\frac{n_{Si}}{n_{Al}} = \frac{100}{\sum_n 0.25 \cdot n \cdot I_{Si(nAl)}}$$: **2.7 (51.9 Al^{fr} / u.c.)**

3.8 (40.0 Al^{fr}/u.c + 11.9 Al^{ex}/u.c.)

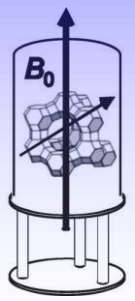

J. Jiao et al., Microporous Mesoporous Mater. 90 (2006) 246.

II. Framework modification

dealumination of zeolite H,Na-Y by steaming

^{27}Al MQMAS NMR spectroscopy (spin I = 5/2) of not hydrated zeolite deH,Na-Y/81.5

B_0 = 17.6 T, ν_0 = 195.5 MHz, ν_{rot} = 30 kHz

n_{Si}/n_{Al} = 6.0 (27.4 Al^{fr}/u.c + 24.5 Al^{ex}/u.c.)

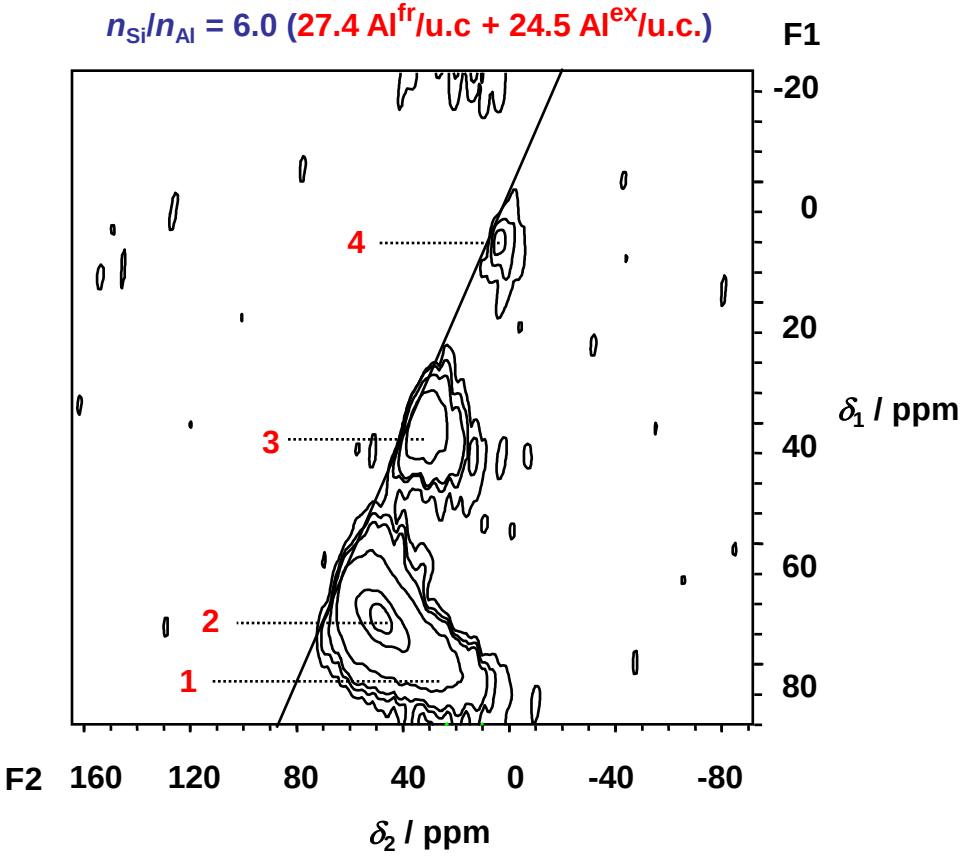

signal 1: Al^{IV}
- $SOQE$ = 15.0±1.0 MHz
- δ_{iso} = 70±10 ppm

signal 2: Al^{IV}
- $SOQE$ = 8.0±0.5 MHz
- δ_{iso} = 65±5 ppm

signal 3: Al^{V}
- $SOQE$ = 7.5±0.5 MHz
- δ_{iso} = 35±5 ppm

signal 4: Al^{VI}
- $SOQE$ = 5.0±0.5 MHz
- δ_{iso} = 10±5 ppm

J. Jiao et al., Phys. Chem. Chem. Phys. 7 (2005) 3221.

III. Tailoring of surface sites

III. Tailoring of surface sites

preparation of dehydrated catalyst samples

vacuum line for dehydration of catalyst samples in glass tubes at elevated temperatures (often 673 K)

transfer of the dehydrated catalyst samples from glass tubes into MAS rotors inside a glove box (dry nitrogen)

III. Tailoring of surface sites

nature of acid sites on zeolites

zeolite Y (FAU, faujasite): supercages connected via 12-ring windows (0.74 nm)

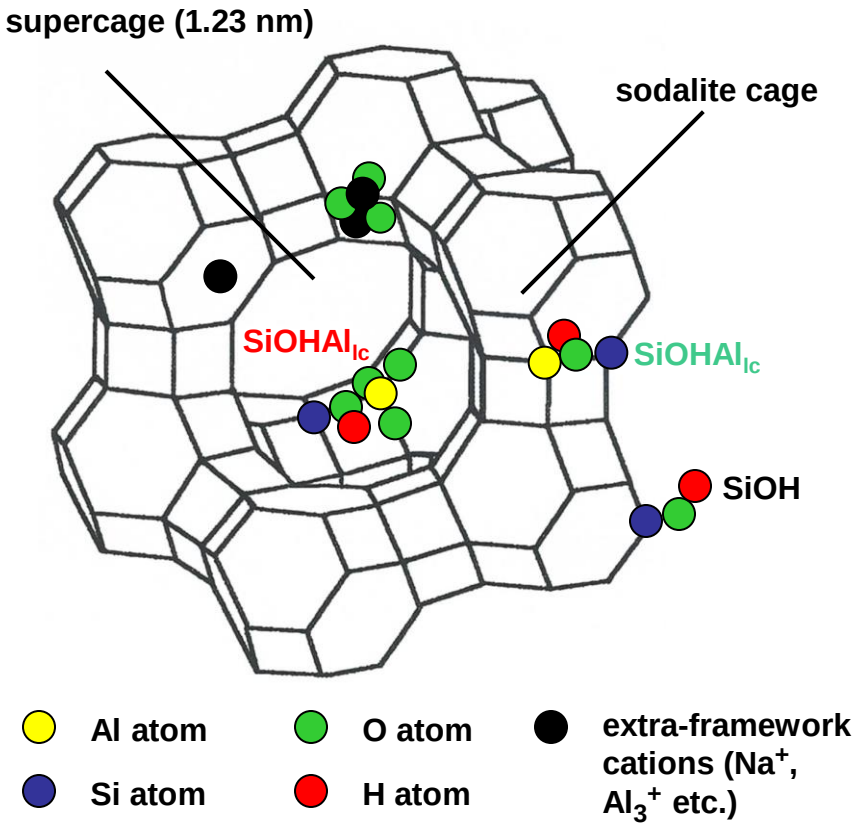

Brønsted acid sites:

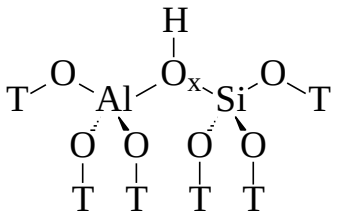

bridging OH group (SiOHAl)

Lewis acid sites:

- framework defects,
- extra-framework species (Al oxide clusters)

III. Tailoring of surface sites

^{1}H MAS NMR chemical shifts of OH groups on solid catalysts

metal OH groups (MeOH), e.g. $MgOH^{+}$, $CaOH^{+}$, $AlOH^{2+}$, $LaOH^{2+}$, etc.

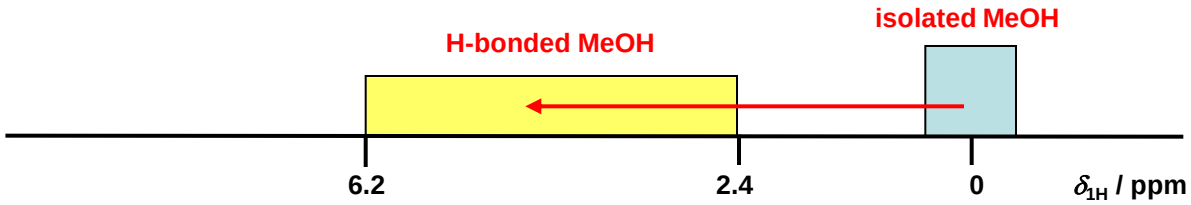

silanol groups (SiOH) at lattice defects and on the outer surface

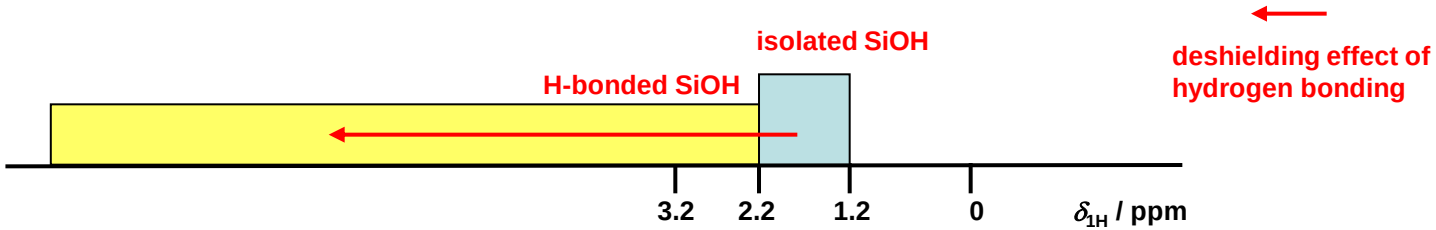

bridging OH groups (SiOHAl) in zeolites

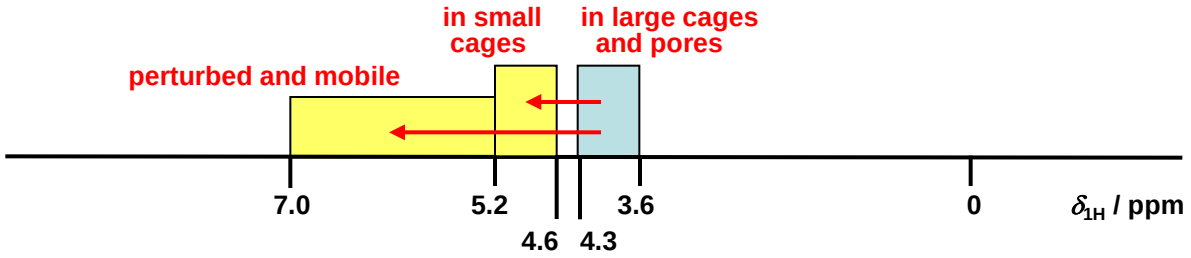

Y. Jiang, J. Huang, W. Dai, M. Hunger, Solid State Nucl. Magn. Reson. 39 (2011) 116-141.

III. Tailoring of surface sites

comparison of the ^{1}H MAS NMR and FTIR spectra of dehydrated zeolite H-ZSM-5 (n_{Si}/n_{Al} = 20)

^{1}H MAS NMR
ν_0 = 800.13 MHz
ν_{rot} = 12 kHz

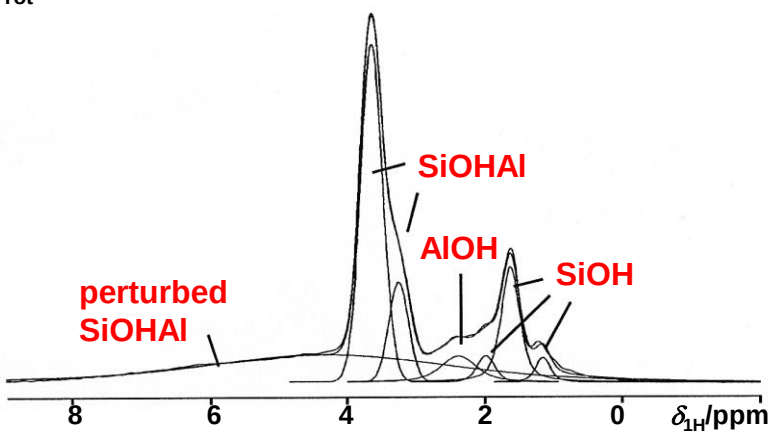

FTIR
Bruker Vector 22

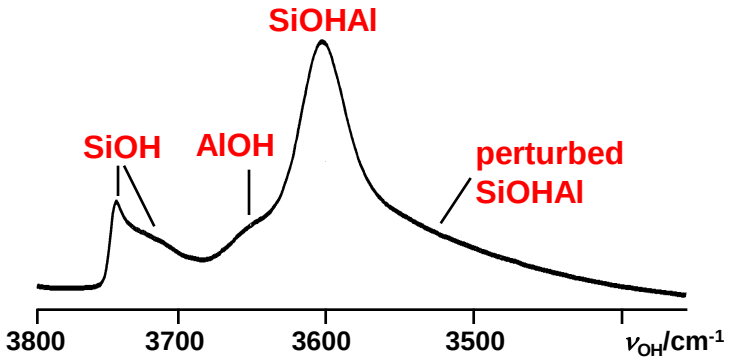

residual ^{1}H MAS NMR linewidths:

SiOH	$\Delta\nu_{1/2}$ = 200 - 400 Hz, 0.5 - 1.0 ppm
AlOH	$\Delta\nu_{1/2}$ = 500 - 600 Hz, 1.2 - 1.5 ppm
SiOHAl	$\Delta\nu_{1/2}$ = 200 - 400 Hz, 0.5 – 1.0 ppm
SiOHAl^{pert}	$\Delta\nu_{1/2}$ ca. 1600 Hz, ca. 4 ppm

III. Tailoring of surface sites

correlation of ^{1}H NMR shift values and FTIR wavenumbers of surface OH groups

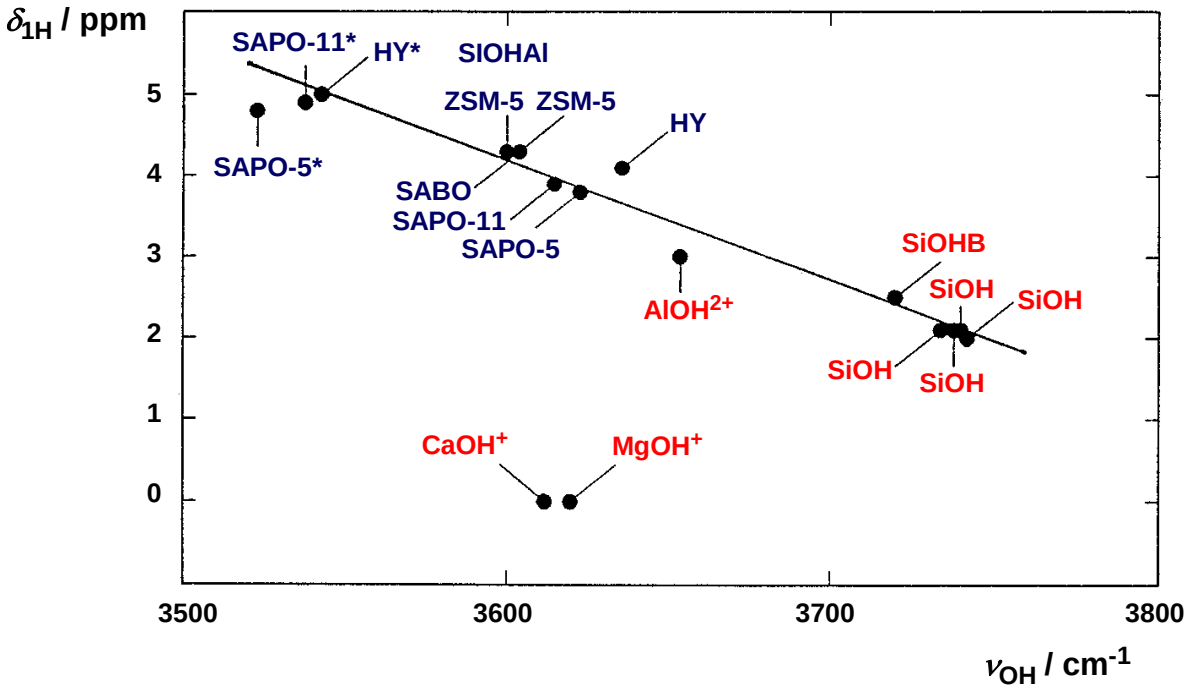

asterisks indicate small cages or pores

E. Brunner et al., Z. Phys. Chem. 176 (1992) 173.

III. Tailoring of surface sites

advantages of FTIR:

- higher sensitivity
- lower costs
- easy adsorption of probe molecules inside the IR cell

advantages of ^{1}H MAS NMR:

- easy sample preparation
- no problems with different particel sizes
- direct determination of OH concentration by signal intensities *)

*) determination of OH concentration n_{OH} by ^{1}H MAS NMR:

- measurement of the intensity of the material under study (I_{OH}) and of an external reference (I_{ref}) with identical parameters (number of scans, receiver gain etc.)
- determination of the weight of the dehydrated sample (m_{OH}) inside to MAS NMR rotor
- calculation of the OH concentration according to:

$$(n_{OH} / g) = (n_{ref} / g) \times (m_{ref} / m_{OH}) \times (I_{OH} / I_{ref})$$

Intensity reference: e.g. dehydrated zeolite 35H,Na-Y with weight m_{ref} and number n_{ref} of hydroxyl groups

III. Tailoring of surface sites

modification of Brønsted acid sites in zeolites *via* steaming

^{1}H MAS NMR

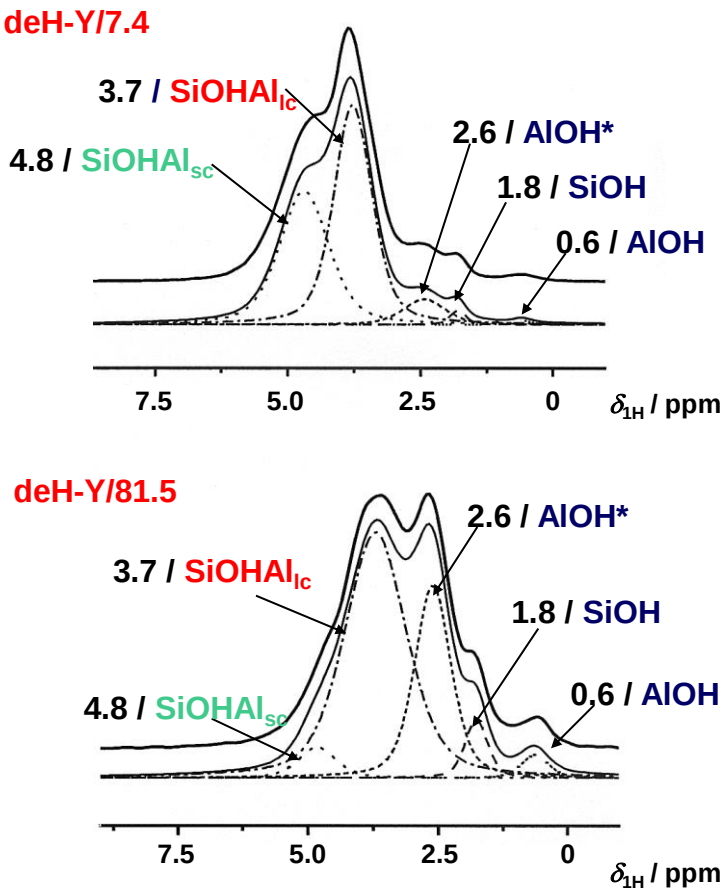

undisturbed metal OH (AlOH) groups:
-0.5 to 0.5 ppm

defect SiOH groups:
1.2 to 2.2 ppm

AlOH* groups at extra-framework Al clusters:
2.8 to 3.6 ppm

bridging OH groups in large cages and pores (SiOHAl$_{lc}$):
3.6 to 4.3 ppm

bridging OH groups in small cages (SiOHAl$_{sc}$):
4.6 to 5.2 ppm

(hydrogen bonded SiOH and SiOHAl groups: 5.2 to 13 ppm)

J. Jiao et al., J. Phys. Chem B. 108 (2004) 14305.

III. Tailoring of surface sites

preparation of Brønsted acid sites in zeolites *via* exchange with multivalent cations

exchange of zeolite Na-Y (n_{Si}/n_{Al} = 2.7) in 0.1 M $Al(NO_3)_3$ solution

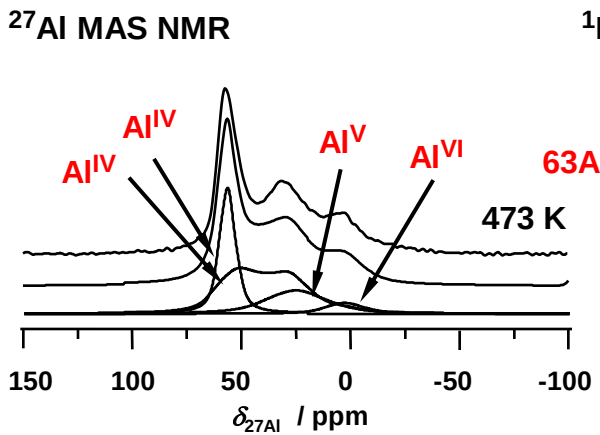

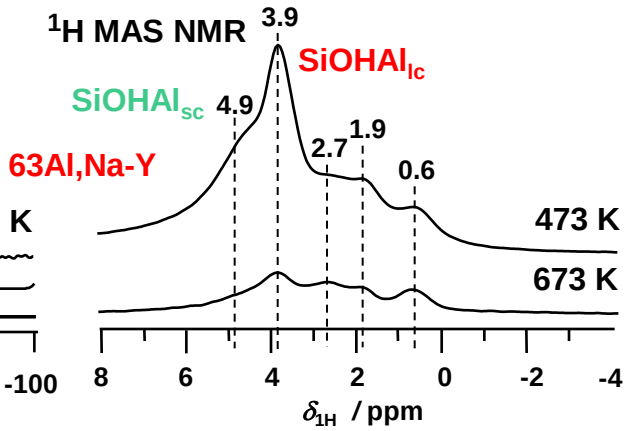

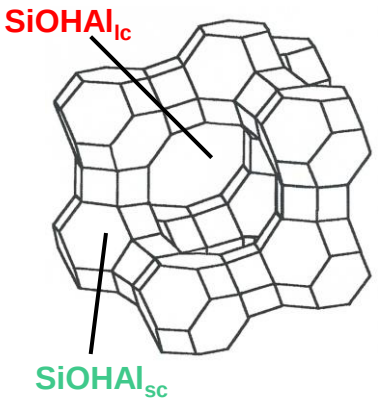

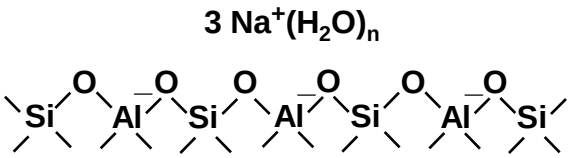

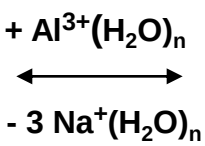

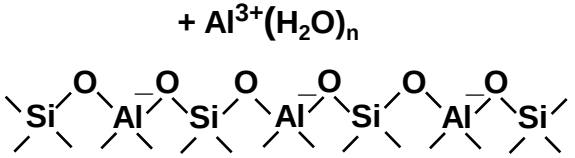

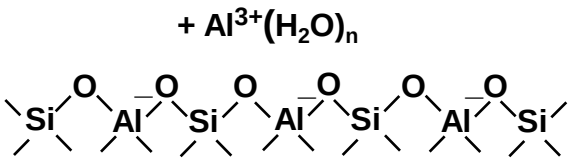

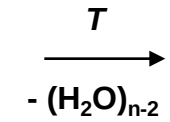

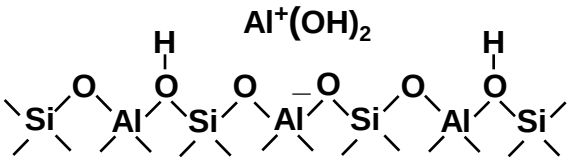

J. Huang et al., J. Phys. Chem. C 112 (2008) 3811.

III. Tailoring of surface sites

Brønsted acid sites in zeolites prepared via exchange with multivalent cations (Al^{3+})

determination of the concentration of OH groups by evaluation of the ^{1}H MAS NMR intensities

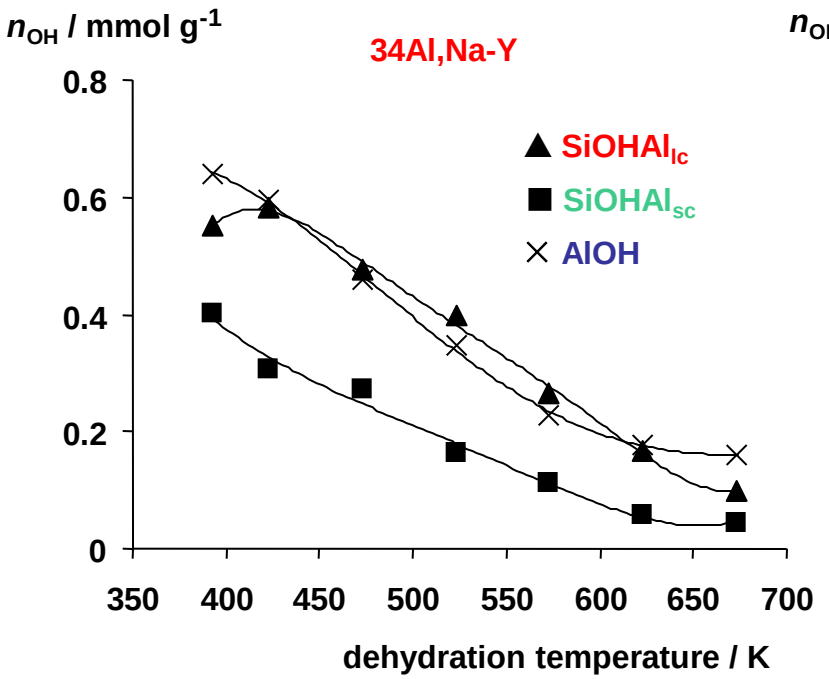

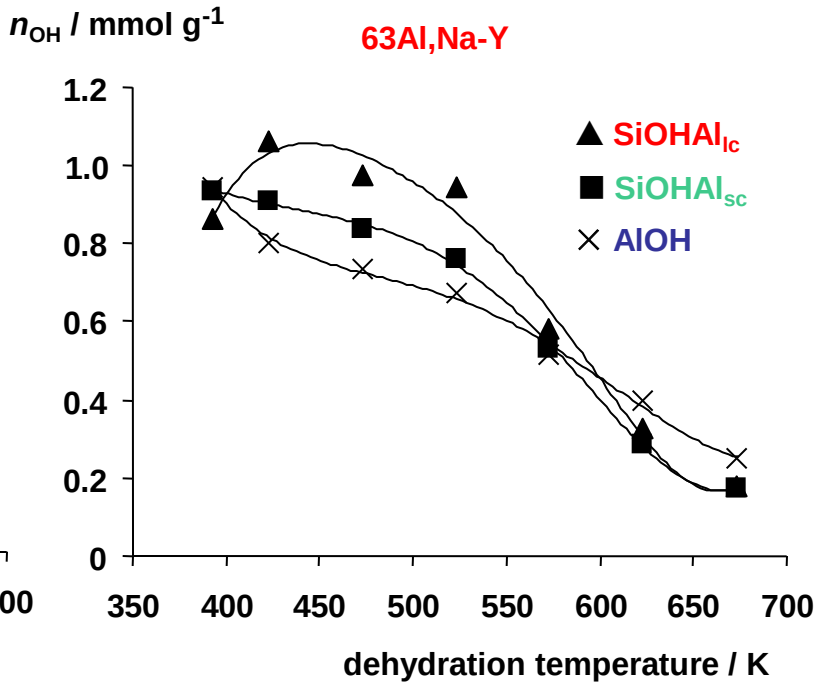

cation-exchange degree and dehydration temperature strongly influence the number of Brønsted sites

J. Huang et al., J. Phys. Chem. C 112 (2008) 3811.

III. Tailoring of surface sites

characterization of the Brønsted acid strength *via* acetonitrile-induced low-field shift $\Delta\delta_{1H}$

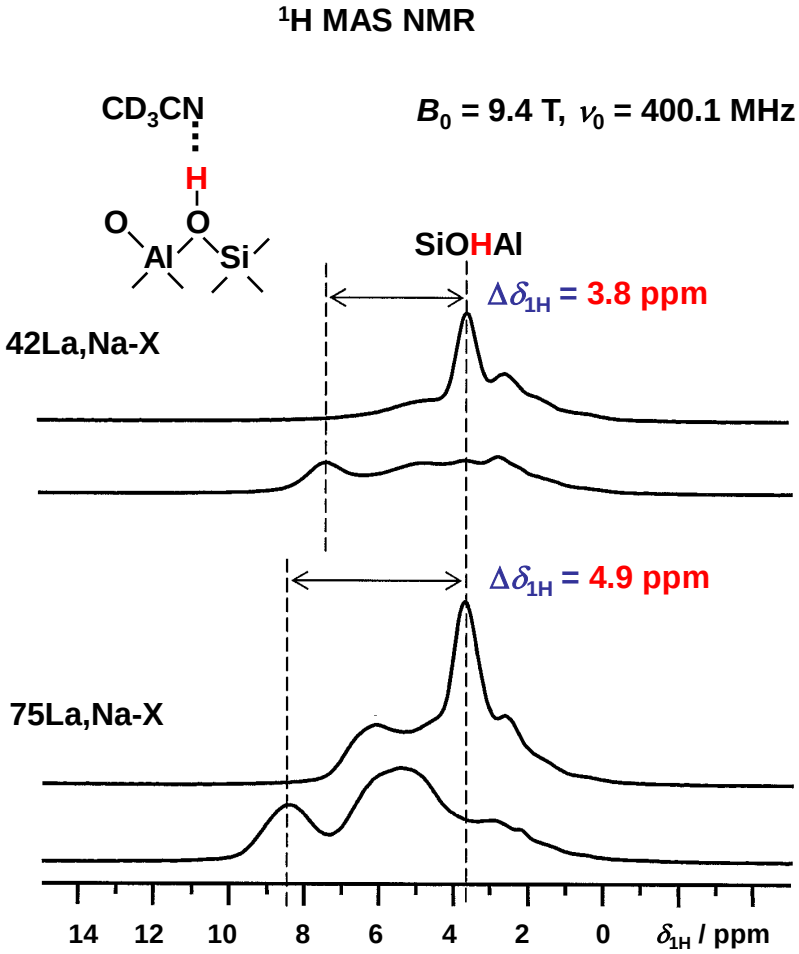

Low-field shift $\Delta\delta_{1H}$	Adsorbent and type of OH group
1.2 ppm	AlOH in MIL-53(Al)
3.6 ppm	H,Na-X (Si/Al= 1.3)
3.8 ppm	42La,Na-X and 32Al,Na-X (Si/Al = 1.4)
4.9 ppm	75La,Na-X (S/Al = 1.4)
5.1 ppm	H,Na-Y (Si/Al = 2.7)
5.3 ppm	34Al,Na-Y and 63Al,Na-Y (Si/Al = 2.7)
5.7 ppm	42La,Na-Y and 75La,Na-Y (Si/Al = 2.7)
6.5 ppm	steamed deH,Na-Y/81.5 (Si/Al = 6)
6.7 ppm	H-MOR (Si/Al = 10)
7.0 ppm	dealuminated H,Na-Y (Si/Al = 18)
7.9 ppm	H-ZSM-5 (Si/Al = 26)

Y. Jiang et al., Solid State Nucl. Magn. Reson. 39 (2011) 116-141.

III. Tailoring of surface sites

characterization of Brønsted and Lewis acid sites *via* ^{13}C-2-acetone as probe molecule

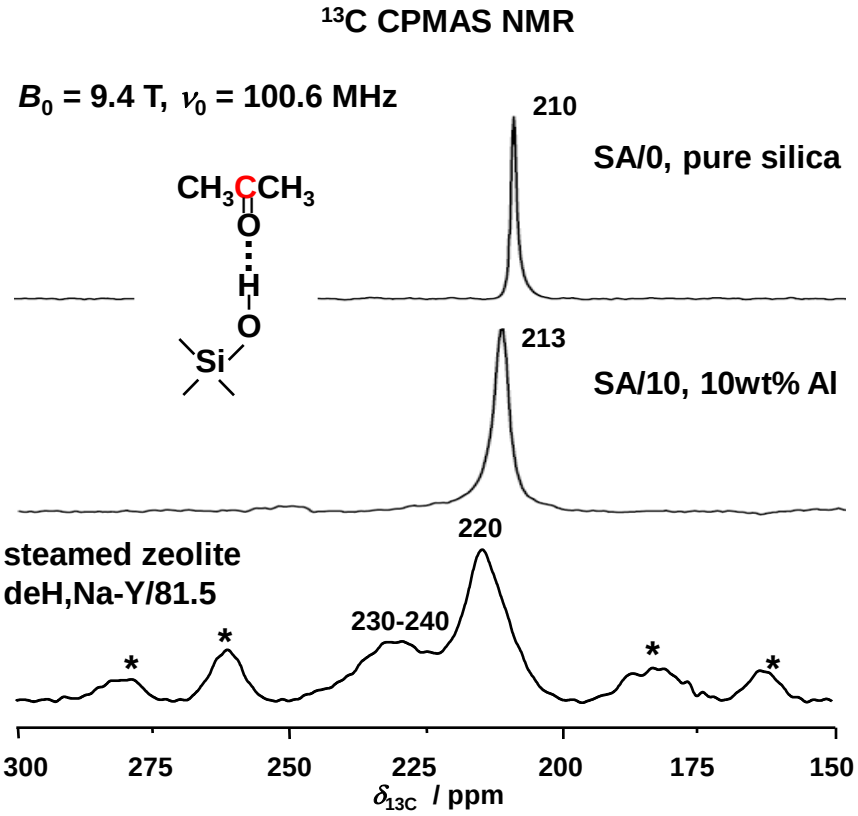

Materials	δ_{13C}	$\Delta\delta_{13C}$
$CDCl_3$	205 ppm	0 ppm
SA/0	210 ppm	5 ppm
SA/10	213 ppm	8 ppm
H,Na-X	215 ppm	10 ppm
SA/70	216 ppm	11 ppm
H,Na-Y	220 ppm	15 ppm
ZSM-5	223 ppm	18 ppm
Lewis sites	230-240 ppm	25-35 ppm

J.F. Haw et al., Accounts of Chemical Research 29 (1996) 259.

Lewis sites formed by steaming

Brønsted sites with different acid strengths (see Tab.)

Y. Jiang et al., Solid State Nucl. Magn. Reson. 39 (2011) 116-141.
H. Fang et al., J. Phys. Chem. C 114 (2010) 12711-12718.

III. Tailoring of surface sites

characterization of Lewis acid sites *via* trimethylphosphine oxide (TMPO) as probe molecule

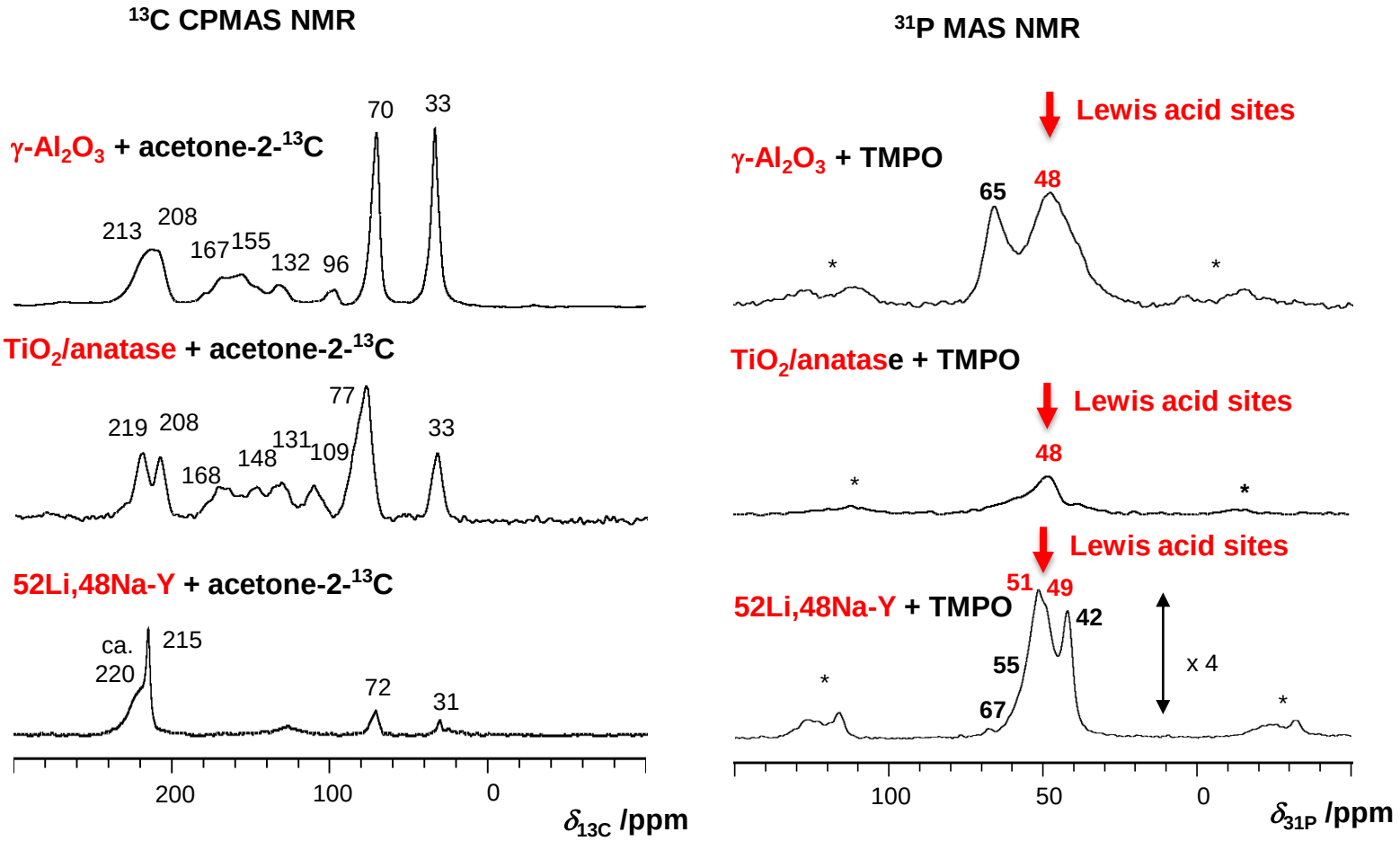

S. Lang, M. Benz, U. Obenaus, R. Himmelmann, M. Hunger, ChemCatChem (2016), DOI: 10.1002/cctc.201600372

III. Tailoring of surface sites

characterization of Lewis acid sites *via* ammonia as probe molecule

^{1}H MAS NMR difference spectra

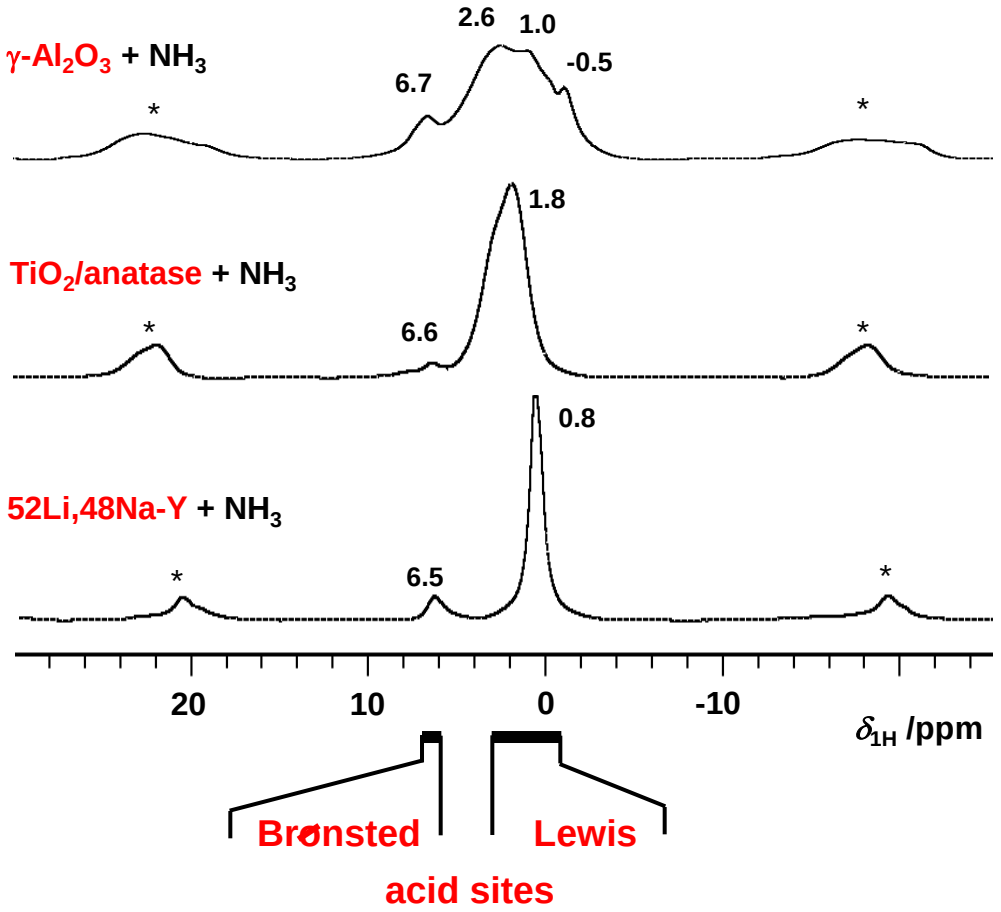

S. Lang, M. Benz, U. Obenaus, R. Himmelmann, M. Hunger, ChemCatChem (2016), DOI: 10.1002/cctc.201600372

III. Tailoring of surface sites

distribution of OH on the outer and inner surface studied by ^{1}H MAS NMR upon loading of perfluorotributylamine (diameter: 0.94 nm)

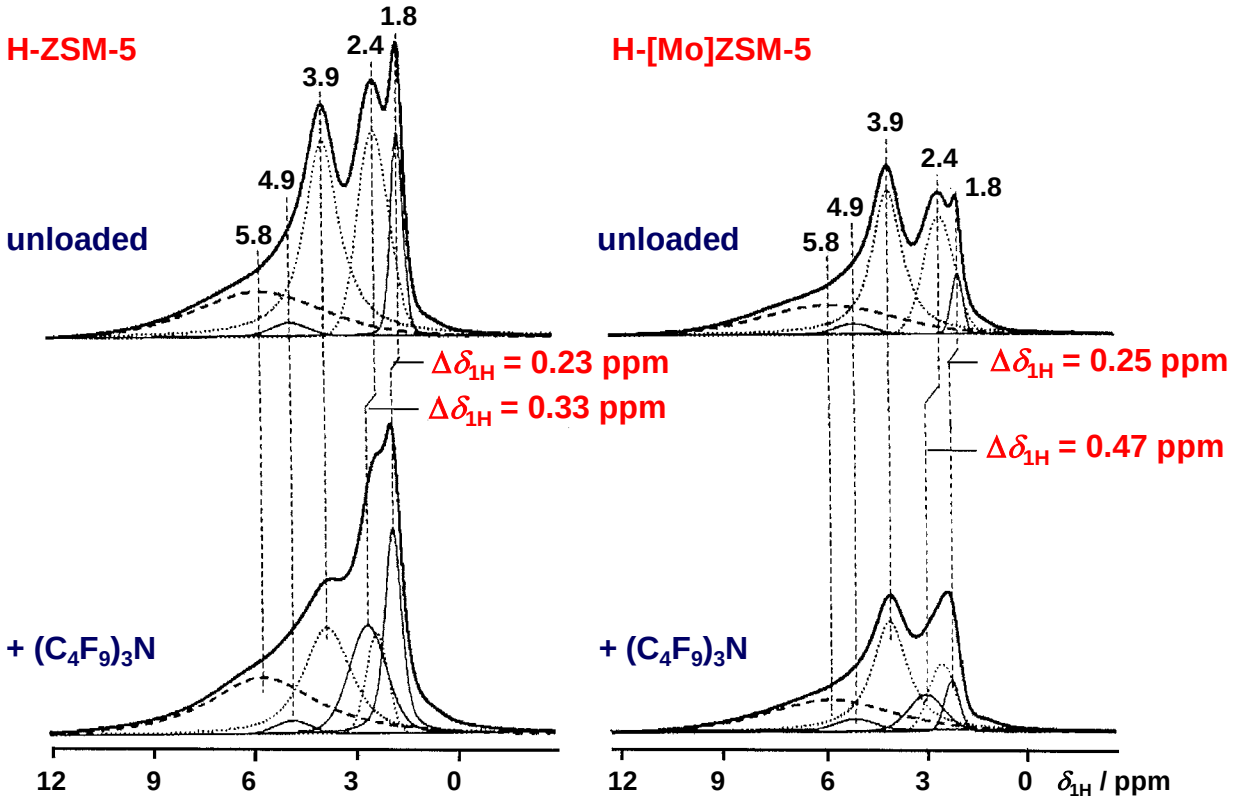

outer surface is exclusively covered by SiOH (1.8 ppm) and AlOH (2.4 ppm) groups with sligthly increased acid strength upon the Mo modification

W. Zhang et al., Chem. Commun. (1999) 1091.

IV. Catalytic investigations

IV. Catalytic investigations

preparation of catalyst samples for *in situ* MAS NMR studies under batch conditions

dehydration and loading of the catalyst inside the glass insert (e.g. commercial Wilmad MAS NMR inserts for 4 mm and 7 mm rotors)

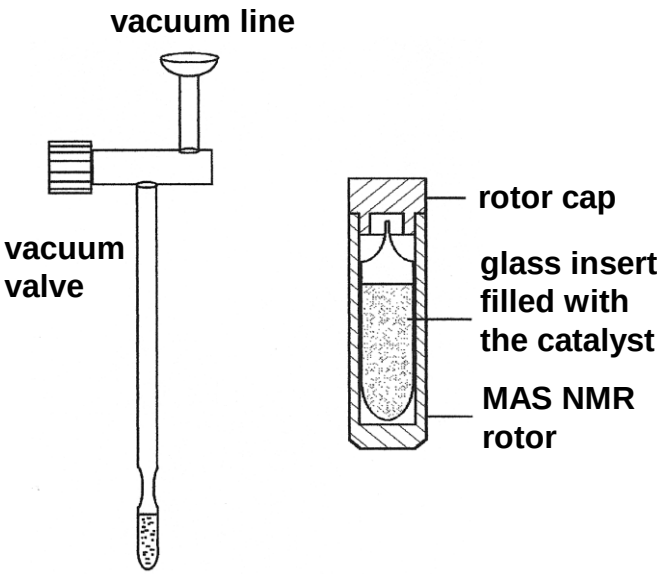

dehydration, loading, and sealing of the catalyst filled in an MAS NMR rotor inside a vacuum equipment

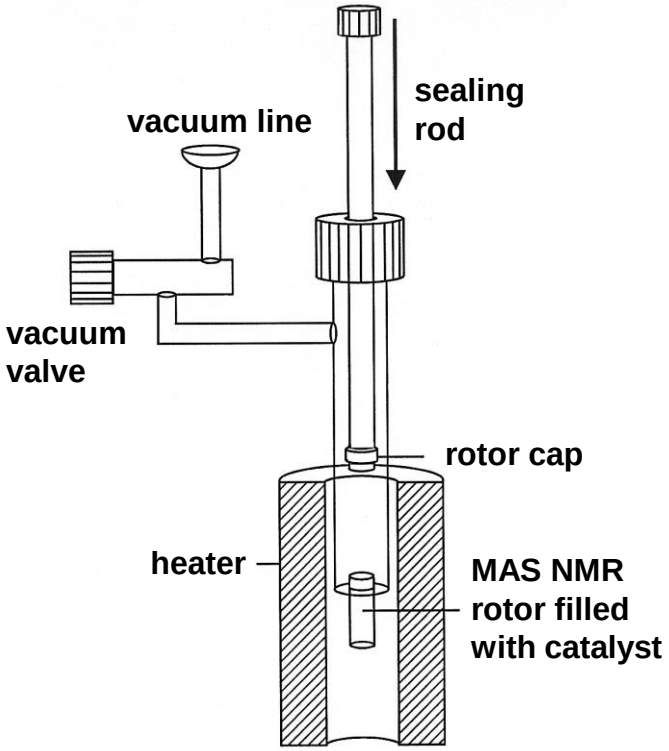

M. Hunger et al., in: B.M. Weckhuysen (ed.), *In situ Spectroscopy of Catalysts*, American Scientific Publishers, Stevenson Ranch, California, 2004, p. 177-218.

IV. Catalytic investigations

preparation of catalyst samples for *in situ* MAS NMR studies under batch conditions

Wilmad insert for 7mm Bruker rotors

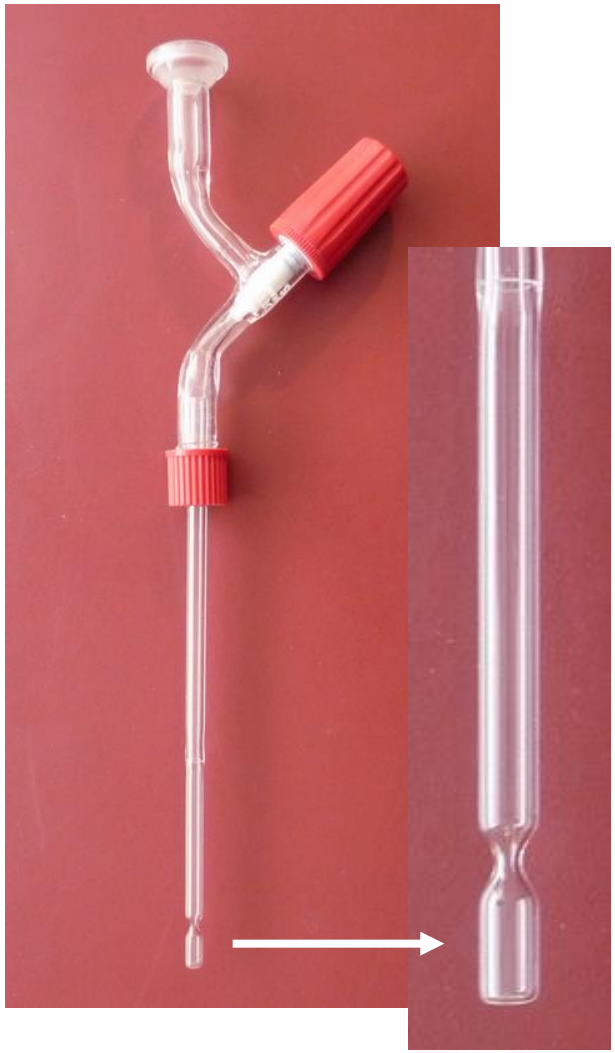

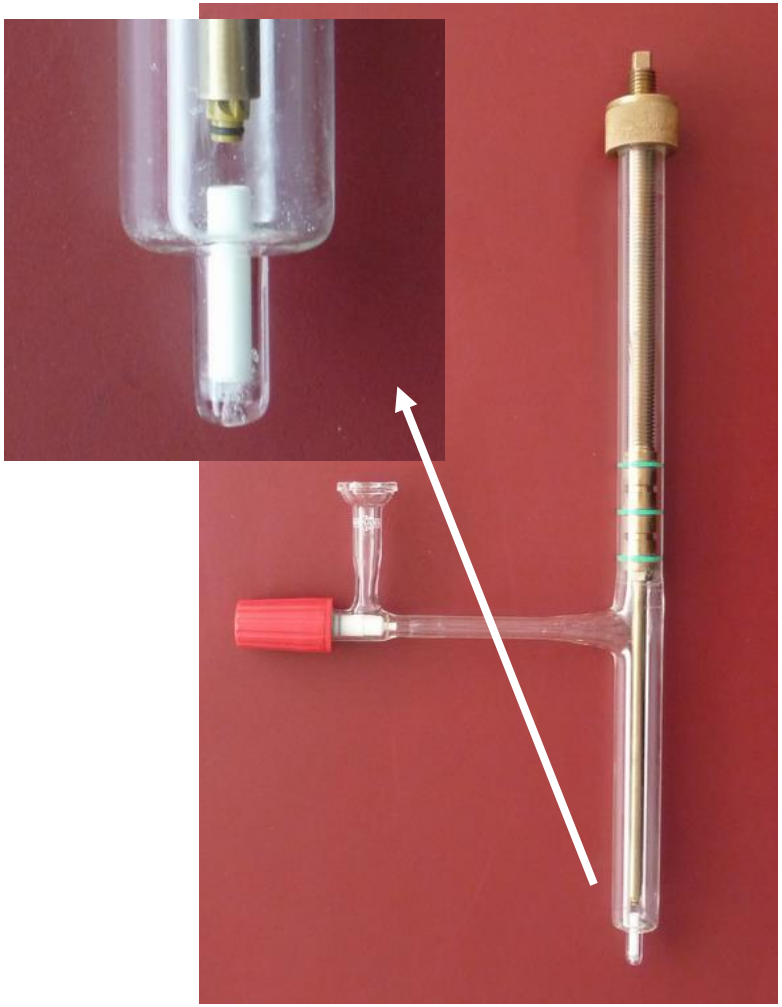

selfmade equipment for rotor sealing

IV. Catalytic investigations

H/D exchange kinetics as an acidity scale

in situ **^{1}H MAS NMR studies of H/D exchange in zeolite H,Na-Y loaded with ethylbenzene ($C_6D_5C_2H_5$)**

stack plot of ^{1}H MAS NMR spectra recorded at *T* = 358 K

B_0 = 9.4 T, ν_0 = 400.1 MHz

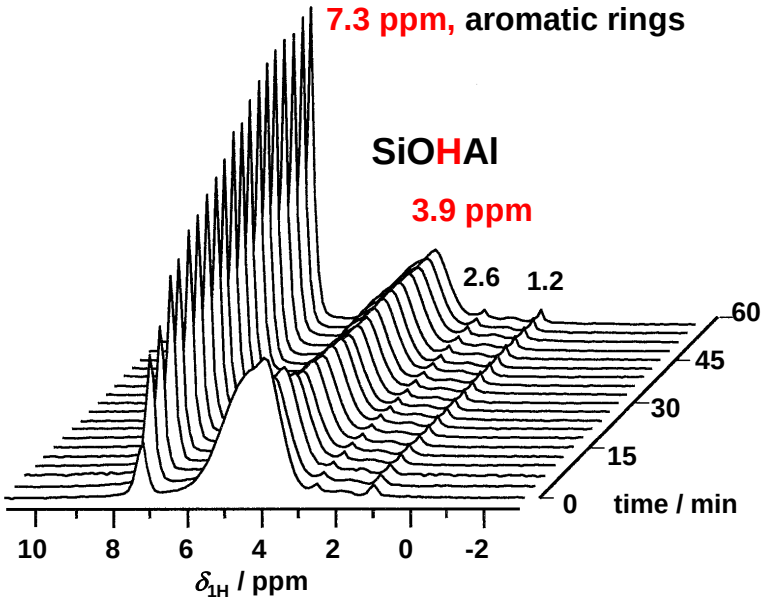

H/D exchange rates at *T* = 328 - 358 K

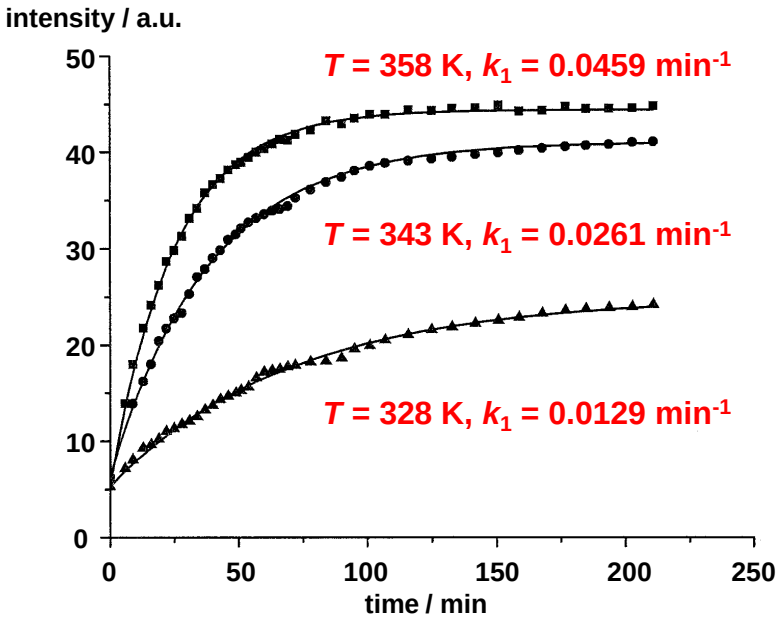

J. Huang et al., Microporous Mesoporous Mater. 99 (2007) 86.

IV. Catalytic investigations

H/D exchange kinetics of alkylated aromatics

in situ **^{1}H MAS NMR spectroscopy of H/D exchange in zeolites H,Na-Y (n_{Si}/n_{Al} = 2.7),**

deuterated aromatics on zeolite H,Na-Y

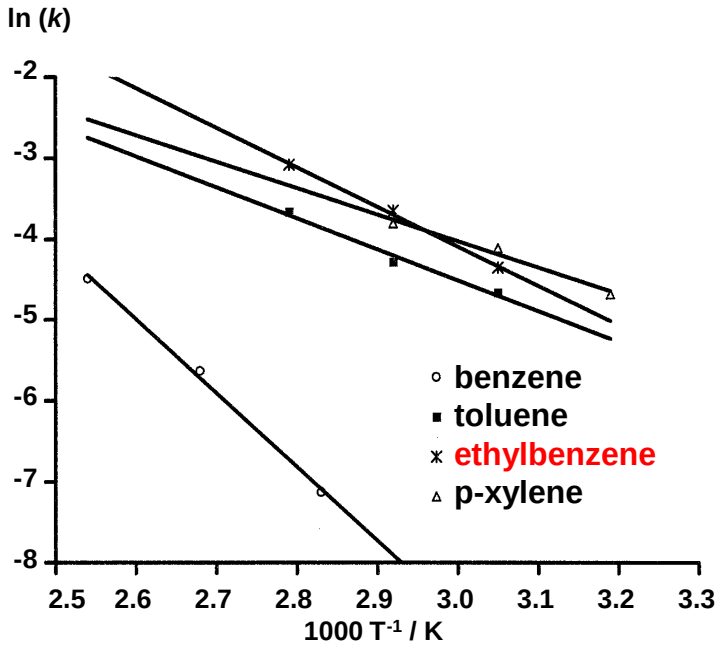

activation energies E_A of H/D exchange with different alkyl-aromatics:

catalyst	molecule	E_A / kJ mol^{-1}
H,Na-Y	benzene	76
	ethylbenzene	41
	toluene	32
	p-xylene	27

J. Huang et al., Microporous Mesoporous Mater. 99 (2007) 86.

IV. Catalytic investigations

H/D exchange kinetics as an acidity scale

in situ **^{1}H MAS NMR spectroscopy of H/D exchange in zeolites H,Na-Y (n_{Si}/n_{Al} = 2.7), 75La,Na-Y (n_{Si}/n_{Al} = 2.7), and H-ZSM-5 (n_{Si}/n_{Al} = 26)**

activation energies E_A of H/D exchange and low-field shifts $\Delta\delta_{1H}$ upon adsorption of CD_3CN:

catalyst	molecule	E_A / kJ mol^{-1}	$\Delta\delta_{1H}$ / ppm
H,Na-Y	benzene	76	5.1
La,Na-Y	benzene	67	5.7
H-ZSM-5	benzene	46	7.9

J. Huang et al., Microporous Mesoporous Mater. 99 (2007) 86.

IV. Catalytic investigations

continuous-flow (CF) MAS NMR technique

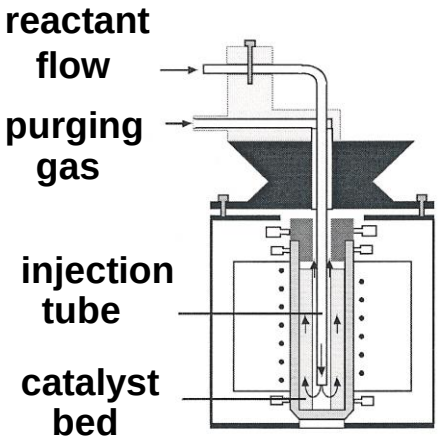

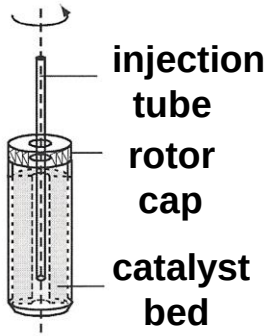

continuous injection of reactants into a spinning MAS NMR rotor reactor

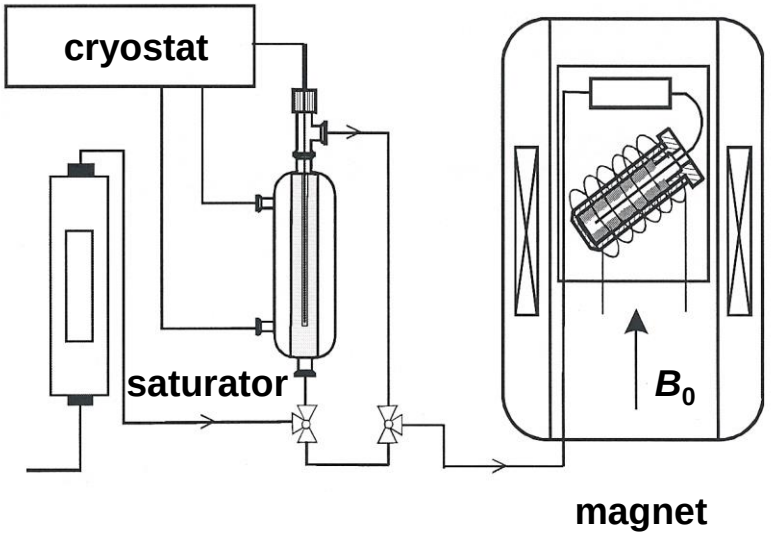

IV. Catalytic investigations

continuous-flow (CF) MAS NMR technique

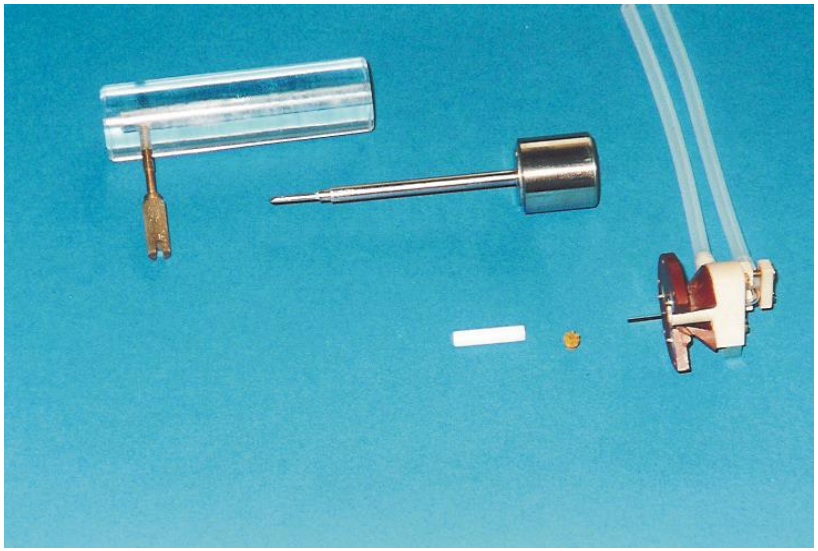

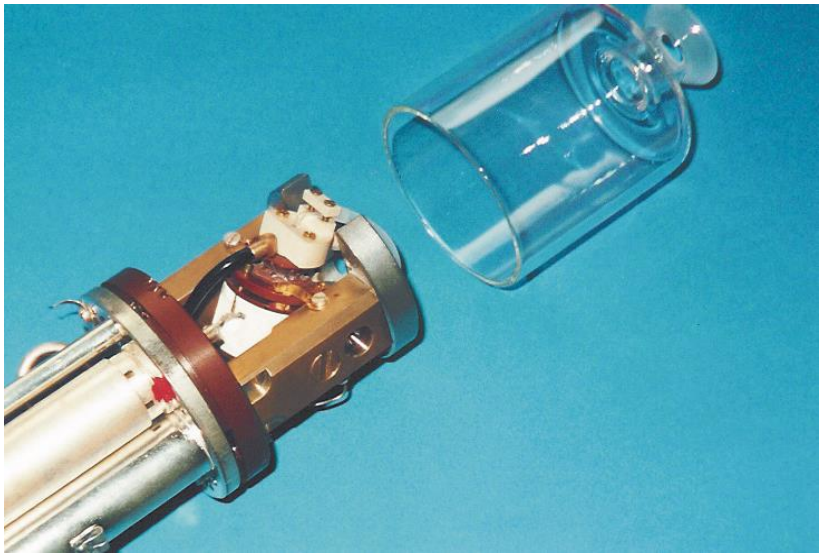

modified 4 mm Bruker MAS NMR probe equipped with an injection system

IV. Catalytic investigations

intrinsic of the hydrogenation rate of acrylonitrile on Pt- and Rh-containing zeolites Y

in situ ^{1}H CF MAS NMR of acrylonitrile hydrogenation on 0.4[Rh]Na-Y at 295 K

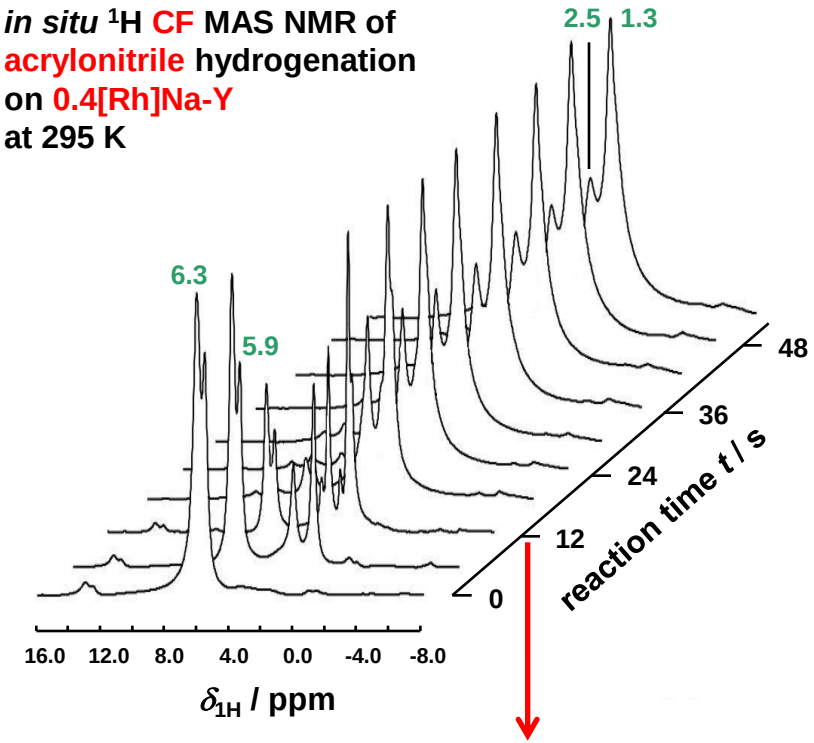

*: formation of half-hydrogenated intermediates?

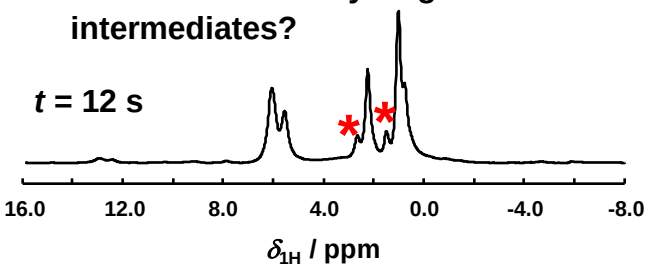

comparison of the intrinsic hydrogenation rates

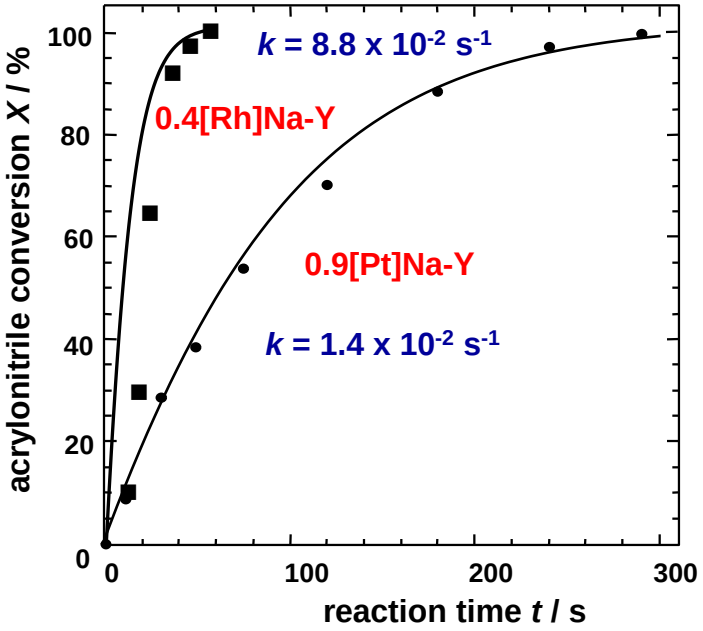

Rh atoms cause a significant higher intrinsic hydrogenation rate compared with Pt atoms dispersed on zeolite Na-Y

H. Henning et al., Micropor. Mesopor. Mater. 164 (2012) 104.
U. Obenaus et al., J. Phys. Chem. C 120 (2016) 2284.

IV. Catalytic investigations

CF MAS NMR of parahydrogen-induced polarization (PHIP)

equipment for *in situ* ^{1}H CF MAS NMR studies of PHIP:

- **at ν_0 = 400.13 MHz, ν_{rot} = 3 kHz, $\pi/4$ pulses, NS = 96, D1 = 0.1 s,**
- **modified Bruker 7 mm MAS NMR probe,**
- **para : ortho ratio of 1 : 1 using a tube filled with FeO(OH) (Sigma-Aldrich) placed in liquid nitrogen,**
- **hydrogen and propene flows of 25 ml/min (1 : 1).**

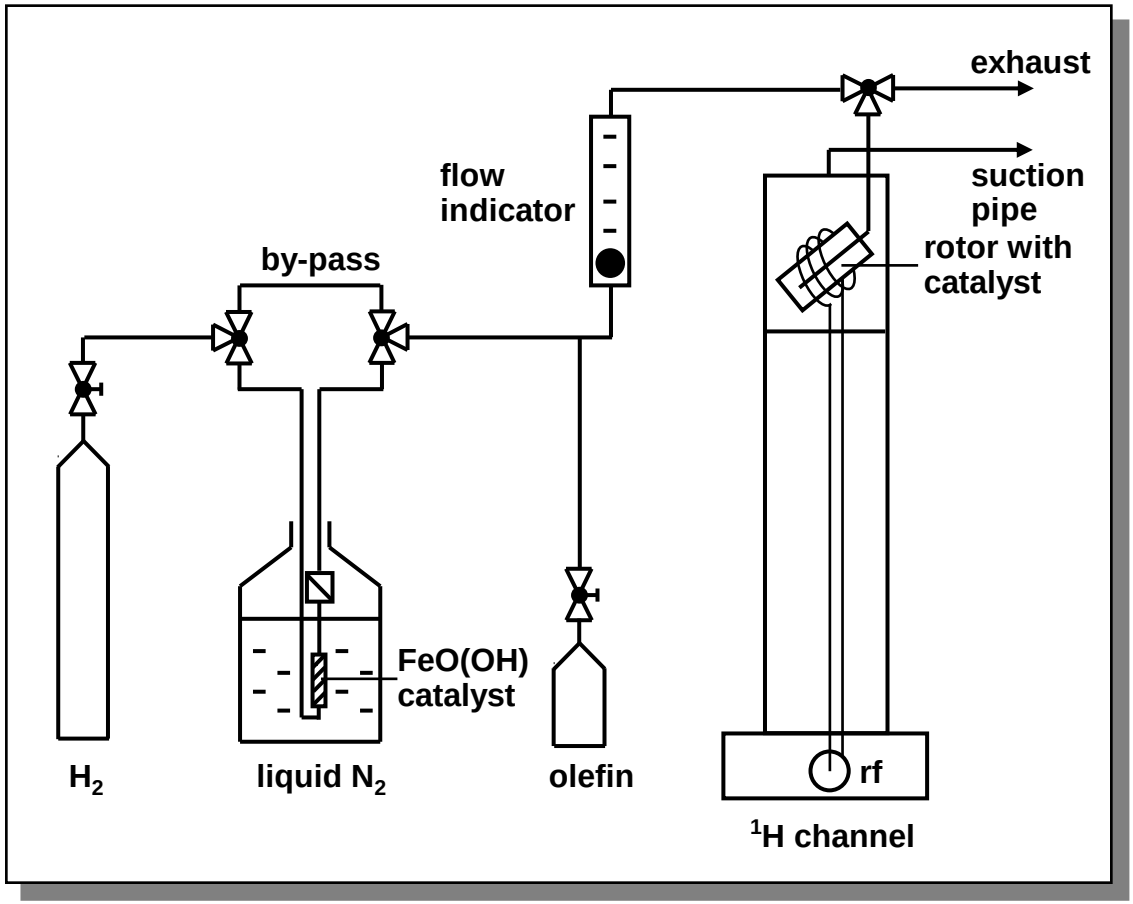

H. Henning et al., Chem. Phys. Lett. 555 (2013) 258.

CF MAS NMR of parahydrogen-induced polarization (PHIP)

PASADENA: Parahydrogen And Synthesis Allow Dramatically Enhanced Nuclear Alignment ($p\text{-}H_2$ incorporation inside the B_0 field)

hydrogenation of propene with para-enriched H_2 **$p\text{-}H_2$:**

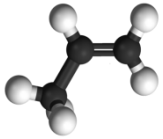

$$CH_3-CH=CH_2 \xrightarrow{+\ p\text{-}H_2} CH_3-CHH-CH_2H$$

- pairwise incorporation of the two H atoms of a $p\text{-}H_2$ causes a large non-equilibrium spin polarization

- ^1H MAS NMR signals due to a pairwise incorporation of $p\text{-}H_2$ into reactants have typical antiphases (see Figure)

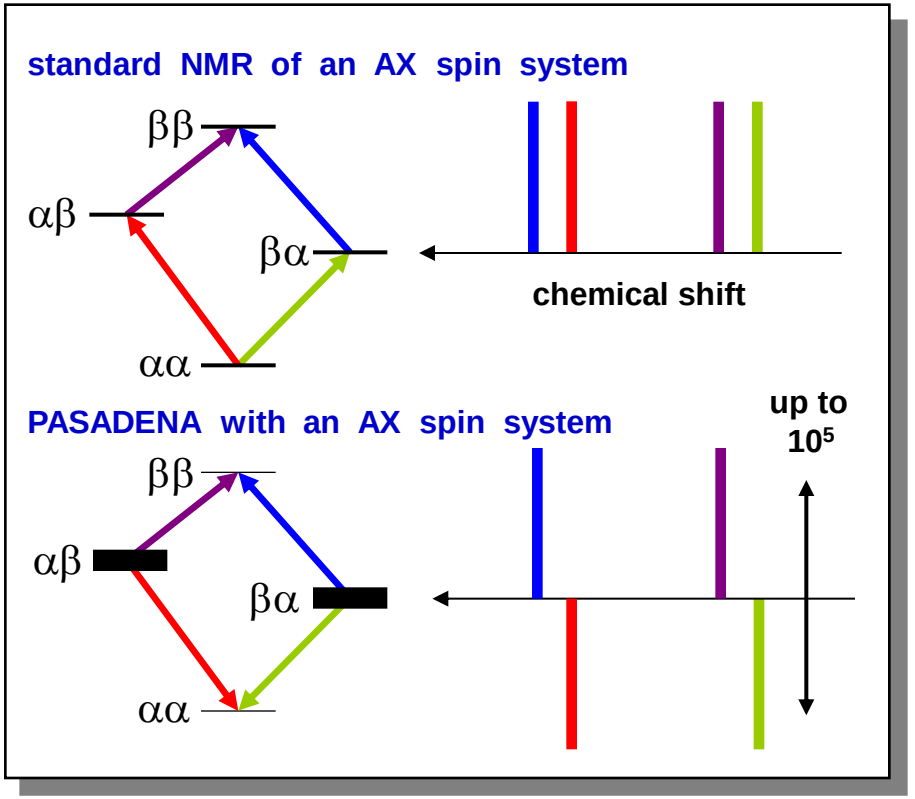

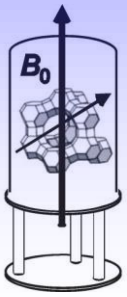

IV. Catalytic investigations

CF MAS NMR of parahydrogen-induced polarization (PHIP)

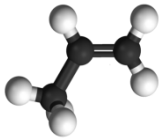

$CH_3-CH=CH_2$ —(+ p-H_2, 0.4[Rh]Na-Y)→ $CH_3-CHH^a-CH_2H^b$

1.72	5.71	4.92		0.91	1.33	0.91

^{1}H NMR shift values

in situ ^{1}H **CF MAS NMR investigation of PHIP at** T **= 295 K**

0.4[Rh]Na-Y (200 mg) + H_2 / propene (1 : 1)

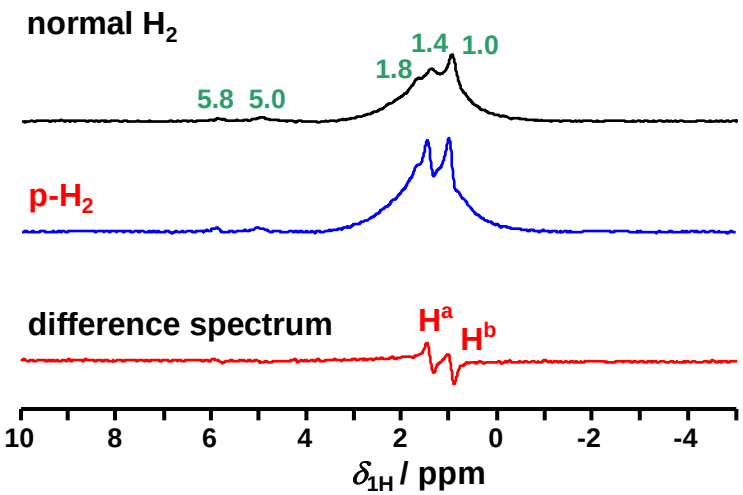

0.4[Rh]Na-Y (35 mg) + H_2 / propene (1 : 1)

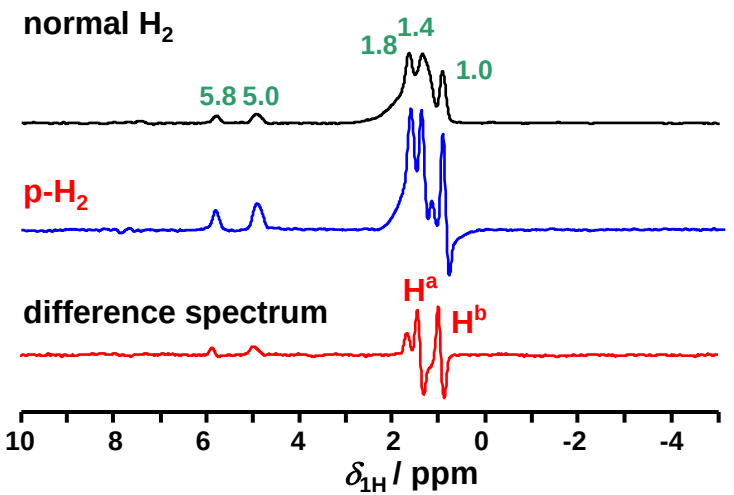

=> pairwise incorporation of p-H_2 into propene on zeolite 0.4[Rh]Na-Y

H. Henning et al., Chem. Phys. Lett. 555 (2013) 258.

Solid-state NMR of solid catalysts

I. Synthesis of catalysts ⟷
- nature and local structure of framework atoms
- framework defects, amorphous phases and impurities

↓

II. Framework modification ⟷
- incorporation and release of framework atoms
- nature and location of extra-framework species and cations
- anchoring of organic compounds

↓

III. Tailoring of surface sites ⟷
- number, strength, and accessibility of Brønsted acid sites
- presence and strength of base sites
- presence of Lewis acid sites

↓

IV. Catalytic investigations ⟷
- adsorbate complexes and intermediates formed on catalysts
- reaction mechanisms
- reasons of catalyst deactivation

↓

topics I to III

Thanks to ….

co-workers:

Thomas Horvath
Michael Seiler
Andreas Buchholz
Udo Schenk
Mingcan Xu
Jiang Jiao
Jun Huang
Yijiao Jiang
Jörg Frey
Reddy Marthala
Wei Wang
Harald Henning
Weili Dai
Zichun Wang
Utz Obenaus
Swen Lang

u.a.

financial support:

Deutsche Forschungs-gemeinschaft

Fonds der Chemischen Industrie

Volkswagen Foundation

DECHEMA e.V.

Alexander von Humboldt-Foundation

u.a.

Thanks to ….